4-30-2015

Comparative Assessment of Hard Palate Thickness Using Micro - CT and Gross Cadaveric Measurements: Implications for the Safe Placement of Orthodontic Miniscrews

Jillian Phillips
Western University, jphil27@uwo.ca

A COMPARATIVE ASSESSMENT OF HARD PALATE THICKNESS USING MICRO-CT AND GROSS CADAVERIC MEASURMENTS: IMPLICATIONS FOR THE SAFE PLACEMENT OF ORTHODONTIC MINISCREWS

(Thesis format: Monograph)

by

Jillian Phillips

Graduate Program in Anatomy and Cell Biology,

A thesis submitted in partial fulfillment
of the requirements for the degree of
Master of Science

The School of Graduate and Postdoctoral Studies
The University of Western Ontario
London, Ontario, Canada

Abstract

The hard palate is a preferred area for orthodontic miniscrew (OMS) insertion due to easy surgical access and favorable anatomical configuration. However, accurate measurement of palatal bone thickness (BT) is crucial for choosing appropriate OMS lengths and insertion sites. The aim of this study is to determine the accuracy of micro-computed tomography (micro-CT) for assessing palatal BT, such that we can determine if it is an objective standard for use in research, to which clinical measurements of BT can be compared.

Ten cadaveric maxillae (54-98 yrs.) were cleaned of soft tissue and imaged using micro-CT imaging. Bone thickness was assessed using grey-scale graphs extracted from the Micro-CT scans at pre-determined sites of interest. The same sites were assessed for BT by gross anatomical means, which entailed measurements of hole depth through the palate following OMS insertion.

Gross anatomical and micro-CT data both revealed a similar trend with BT thinning from anterior to posterior. Although no statistically significant differences were found between measurements differences on a site-by-site basis, the suitability of micro-CT as an imaging tool for hard palate assessment could not be determined due to limitations in the gross anatomical protocol.

Based on gross anatomical measurements, orthodontic miniscrew insertion is deemed appropriate in the anterior palate and paramedian region.

Keywords

Hard palate, micro-CT, bone thickness, gross anatomy, miniscrew, orthodontic miniscrew, cadaver.

Acknowledgments

It is with sincere gratitude that I would like to acknowledge the following individuals for their contributions to this project and/or for enriching my journey through the Clinical Anatomy program.

Many thanks to my collaborator Dr. Carine Bourassa and our co-supervisor Dr. Ali Tassi for making this project possible. Your combined clinical knowledge and critical thinking have been assets to shaping the project. Thank you for Carine for providing valuable critical opinions and insight and for encouraging me to challenge myself. Dr. Tassi, thank you for providing materials for the completion of the project and for expressing your valuable suggestions along the way.

A big thank you to my primary supervisor Dr. Khadry Galil for making this project possible and for supporting me in many ways throughout. Thank you for remaining positive in the face of roadblocks, generating excitement about the research and always encouraging me to succeed. Your support and infectious humor have made the journey both memorable and enjoyable.

A huge thank you to my advisor Dr. Yara Hosein for your continuous support, encouragement, and willingness to spend long hours tackling roadblocks and assisting with data analysis and interpretation. Your expertise in research and superb critical thinking have been invaluable. This work would not be what it is today without your guidance.

To my advisor Dr. Katherine Willmore, thank you for your willingness to meet and help tackle challenges along the way and for your constant encouragement and provision of a space to work in the 'Willmore lab'. Your positive energy has motivated me along the way and your critical thinking has not only guided my decisions throughout the project but has forced me to constantly challenge myself. For that I am grateful.

To Dr. Marjorie Johnson, thank you for accepting me into the Clinical Anatomy program. At the outset I had little anatomical knowledge but I am leaving with a plethora of knowledge and skills, for which I owe many thanks to you and the instructors of the program. Thank you for being the 'rock' of my research committee and our program in general, always providing an objective view, critical suggestions for improvements, and for always being warmly welcoming when I reached out to you.

A large thanks to Ormco for their generous donation of VectorTAS^{TM} orthodontic miniscrews used both in this project and by my collaborator.

Another set of recognition goes out to Haley Linklater and Kevin Walker in the gross anatomy lab, for their help with specimen acquisition and to Mahdi Moslim, dentistry technician for his innovative efforts in apparatus design. Kevin, thank you for the countless hours you spent helping me in the lab; your company and humor certainly made the long hours in lab both memorable and more enjoyable. Haley, thank you for all the

opportunities to get involved with educational outreach sessions; these provided valuable practice in teaching anatomy and helped solidify my learning.

I would also like to recognize the undergraduate students who assisted with the study. To my second rater, Heba Almadhoun, thank you for the immense amount of time and effort you've dedicated to this project both with micro-CT measurements (from the previous protocol) and the long hours you spent taking physical measurements in the lab. I commend you on your ability to manage your time so well a heavy course load, a child at home, and all the work you've taken on with this study! To Ashraf Altesha, thank you for your assistance in the anatomy lab and for your work graphically representing the early data. It was a pleasure working with both of you and I wish you both great successes in your future studies!

Another set of thanks goes to the Team at Robarts Research Institute, led by Dr. Holdsworth. Thank you to Jopeph Umoh for specimen scanning micro-CT reconstruction. Another thanks goes to Steve Pollmann who indirectly assisted in this study by creating the program used for micro-CT analysis by Dr. Bourassa.

Thank you to Dr. Brian Allman and his graduate student Tyler Beveridge for providing the surgical microscope/digital camera, and assisting with its setup, respectively. Another thanks to Tyler for your help selecting statistical tests and your input on the design of apparatuses intended for the original protocol.

To My Clinical Anatomy classmates, thank you for making my time in the program enjoyable, for being my unwavering support and encouragement and for your willingness to listen to and discuss any issues I was tackling. It has been a pleasure working with you and I have learned so much from the diverse skills you all brought to the program. I wish you all great success in your future studies and careers.

To my family, although most of you are a distance away, you remain rock in terms of support. I thank you for always lending a supportive ear when needed and for instilling in me the value of higher education. Your constant encouragement and support has been the foundation of my successes.

Lastly, and most importantly I would like to recognize the donors and their families who supported their decision to donate; this research would not have been possible without your gracious gift to the university. I am humbled by your selfless act of body donation and would like to personally thank you for providing this learning opportunity for me. In light of your generous gift, I can only assume that you cared about the education of our students and the impacts of medical and/or dental research toward a brighter future. Thank you for your trust and investment in us.

Table of Contents

Abstract ii

Acknowledgments iii

List of Tables vii

List of Figures viii

List of Appendices x

1 Introduction 1

1.1 Anatomy of Interest 1

1.1.1 Maxillae 1

1.1.2 Location and Basic Anatomy of the Palate 2

1.1.3 Bony Composition of the Hard Palate 3

1.1.4 Foramina, Nerves and Vessels of the Palate 4

1.2 Orthodontic Miniscrews 7

1.3 Imaging Modalities: CT and Micro-CT 10

1.4 Literature of Interest 11

1.5 Purpose of Study 13

1.6 Hypothesis 13

2 Materials and Methods 14

2.1 Specimen Selection and Exclusion Criteria 14

2.2 Maxilla Isolation, Preparation and Storage 15

2.3 Selection of Measurements Sites 18

2.4 Micro-CT Imaging and Bone Thickness Analysis 19

2.5 Gross Anatomical Measurements and Validation 21

2.5.1 Measurements Validation 21

2.5.2 Gross Anatomical Measurements 26

2.6 Statistical and Graphical Analysis 29
3 Results 32
3.1 Validation Study Findings 32
3.2 Descriptive statistics 33
3.3 Reliability Between Physical Measurements 33
3.4 Correlations 35
3.5 Measurement Agreement 37
4 Discussion 45
5 Conclusions 50
6 References 51
Appendices 60
Curriculum Vitae 80

List of Tables

Table 1- Average Percent Error Associated with Measurements.....32

Table 2 - Descriptive Statistics for Measurement Differences by Site.....33

Table 3 - Outlying Measurements and Visual Inspection of Site.....41

Table 4 - Percent Differences between Micro-CT and Anatomical Measurements.....42

List of Figures

Figure 1 - Location and Structure of the Human Maxillae…….....1

Figure 2 - Location of the Human Palate …… …….....3

Figure 3 - Bony Composition of the Hard Palate, Inferior View……...…....4

Figure 4 - Typical Incisive Canal and Foramen 5

Figure 5 - Distribution of Arteries and Nerves to the Hard Palate 6

Figure 6 - Orthodontic Miniscrews of Various Designs…….....……..…….8

Figure 7 – Location of band saw cuts for palate isolation.....15

Figure 8 - Isolated Maxilla Following Gross Anatomical Dissection.....16

Figure 9 - Specimen embedded in Acrylic Following Teeth Removal.....17

Figure 10 – Specimen Following OMS Insertion, Indicating BT Measurement Sites.....19

Figure 11 - Micro CT Scanning of Specimens, Robarts Research Institute.....20

Figure 12 - Cedar Wedges Used for Measurement Validation.....22

Figure 13 – 'Gold Standard' Caliper Measurement Used for Measurement Validation...23

Figure 14 - Insertion of Orthodontic Miniscrews into Cedar Wedge.....24

Figure 15 - Marking of Dissection Pin for Depth Measurement.....25

Figure 16 – Setup and Standardization for Anatomical Measurements.....26

Figure 17 - Isolated Specimen Following Acrylic Removal.....27

Figure 18 – Preparation of Specimen for Physical Measurements, Superior view.....28

Figure 19 - Intra-rater Reliability for Rater One BT Measurements.....34

Figure 20 – Inter-rater Reliability for Rater one and Two BT Measurements.....35

Figure 21- Relationship between Micro-CT and Rater 1 Physical Measurements of Palate BT.....36

Figure 22- Relationship between Micro-CT and Rater 2 Physical Measurements of Palate BT.....37

Figure 23 - Agreement between Micro-CT and Gross Anatomical Measurements, Assessed with Traditional Bland-Altman Plot.....39

Figure 24 - Agreement between Micro-CT and Gross Anatomical Measurements Assessed with Modified Limits of Agreement.....40

Figure 25 - Comparison of Median BT Values Reported by Micro-CT and Physical Measurements.....43

Figure 26 - Mean Anatomical Bone Thickness by Site..... 44

List of Appendices

Appendix A – Permissions to Scholarship@Western 61

Appendix B - Rights and Permissions 62

Appendix C: Specimen Information 71

Appendix D: Sites Extended with a 12mm OMS 72

Appendix E: Averaged Measurements and Percent Errors for 73

Appendix F: Bone Thickness Measurements 74

Appendix G: SPSS® Output - Tests of Normality 78

Appendix H: SPSS® Output - Kruskal Wallis H Test 79

1 Introduction

1.1 Anatomy of Interest

1.1.1 Maxillae

The paired maxillary bones, also known as maxillae, form the upper jaw of the human skull and house the upper dentition or teeth (Figure 1). Each maxilla is an irregularly shaped bone, consisting of a hollow body (the main bulk of the bone) with four extensions: the alveolar, frontal, palatine, and zygomatic processes (Berkovitz, Moxham, & Holland, 2009; Scheid & Weiss, 2012). The region of the maxillae that is of interest to this research project are the palatine processes, which together constitute the majority of the hard palate (Scheid &Weiss, 2012).

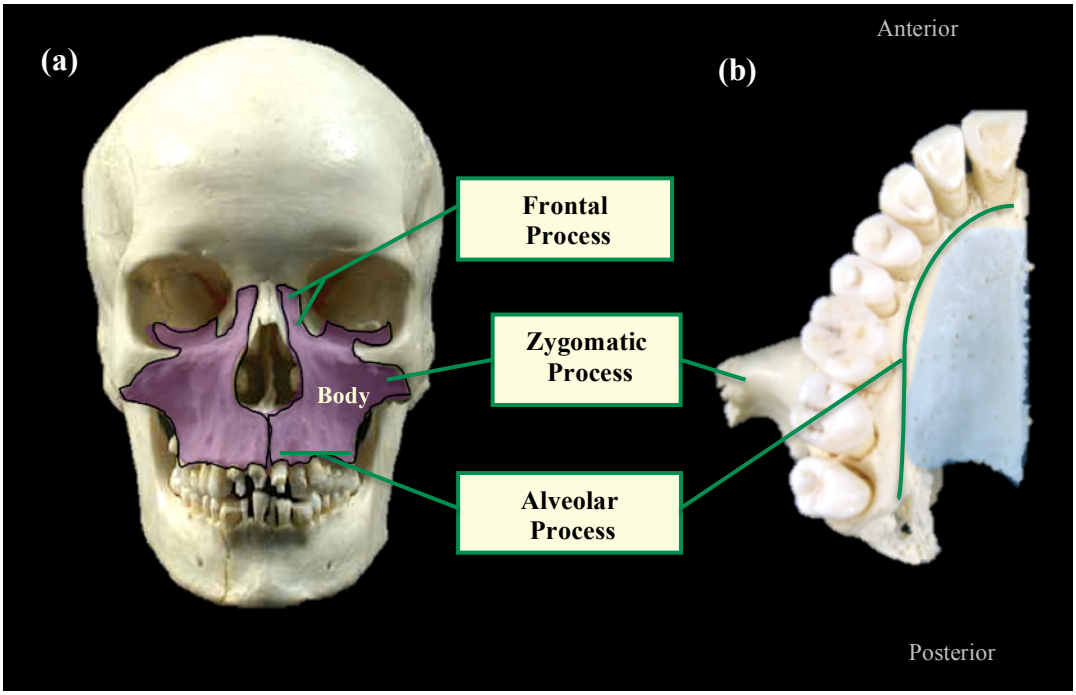

Figure 1 - Location and Structure of the Human Maxillae*

(a) Frontal (anterior) view of human skull with paired maxillae highlighted in purple
(b) Inferior view of isolated human maxilla, with palatine process highlighted in blue

*Reprinted and modified with permission from Galil (2004), http://www.forestcity.ca/drgalil/skull/index.htm

1.1.2 Location and Basic Anatomy of the Palate

The human palate or roof of the mouth is comprised of two parts: the *hard palate*, which forms the anterior two-thirds (and therefore the bulk of the palate) and the *soft palate*, which includes the remaining third (Figure 2). The hard palate is a bony structure overlaid by keratinized mucosa (mucous membrane), forming the rigid, arched, anterior roof of the oral cavity, separating it from the nasal cavities above (Day & Girod, 2006; Scheid & Weiss, 2012). The bones of the palate are lined externally with a layer of periosteum, a dense fibrous connective tissue layer, which tightly attaches to the overlying palatal mucosa (Berkovitz et al., 2009; Day & Girod, 2006; Ross & Pawlina, 2011). The mucosa in the posterior third of the hard palate contains numerous small *palatine glands* which secrete saliva, whereas the anterior portion of the hard palate as well as the midline contain firm ridges of mucosal tissue, the *palatine rugae* (anteriorly) and the *palatine raphe* (midline), which lack underlying glands. The palatine raphe overlies the median palatine suture (discussed later) and is continuous with the *incisive papilla*, an anterior bump of mucosal tissue overlying the incisive foramen (Scheid & Weiss, 2012). The soft palate, although continuous posteriorly with the mucosa of the hard palate, lacks underlying bone structure. Rather, it is a fold of mucous membranes or mucosa overlying contributing musculature and a thick aponeurosis (a broad, flattened tendon-like structure), separating the oral cavity from the nasopharynx (Berkovitz et al., 2009; Day & Girod, 2006; Norton, 2012; Scheid & Weiss, 2012). Given its lack of bone, and this thesis' focus on the bone thickness of the palate, the soft palate is not of interest to the current study and will not be discussed further.

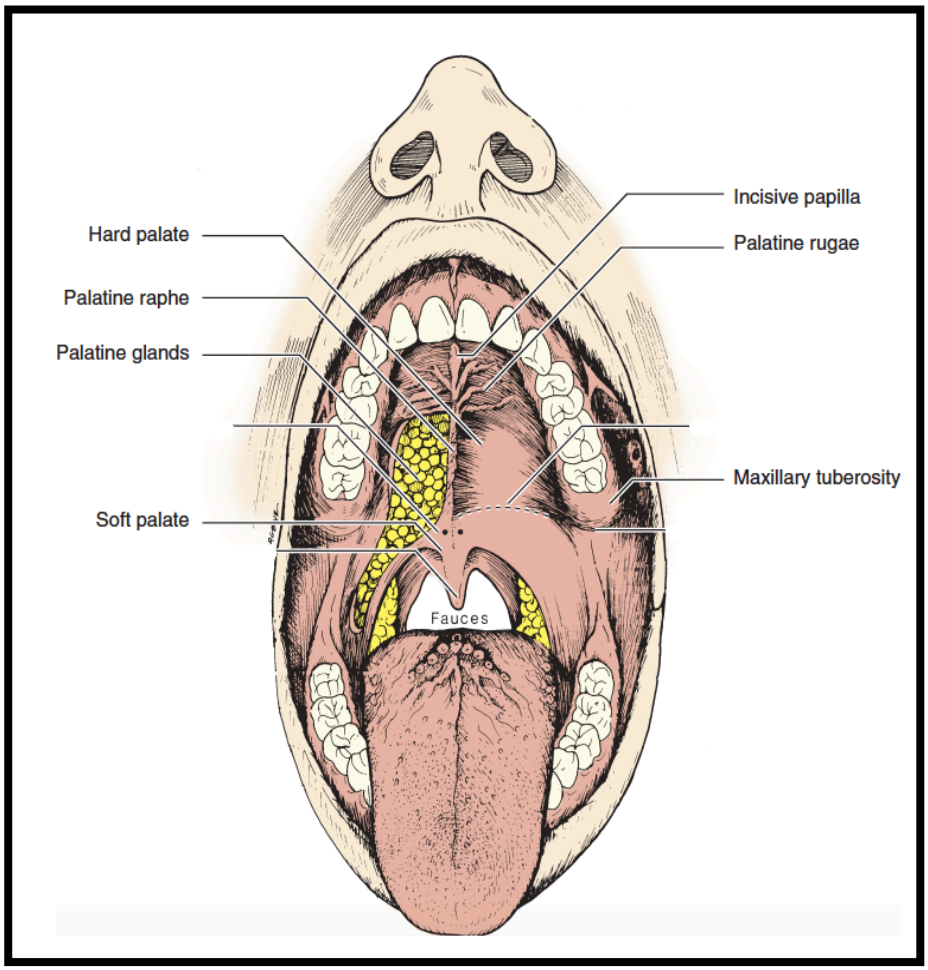

Figure 2 - Location of the Human Palate*

* Reprinted from Woelfel's Dental Anatomy 8th Ed, by Scheid. & Weiss, G. (2012), with permission from Lippincott, Williams & Wilkins

1.1.3 Bony Composition of the Hard Palate

Anatomically, the skeletal or bony portion of the hard palate is composed of the bilaterally paired palatine processes of the maxilla and the bilaterally paired horizontal plates of the palatine bones (Figure 3). Medially, these bones come together at the midline, forming the median palatine suture, also known as the intermaxillary suture. A second suture or point of fusion within the hard palate is the *transverse palatine suture* or

palatomaxillary suture, located between the horizontal plates of the palatine bones and the palatine processes of the maxillae (Scheid & Weiss, 2012). The alveolar process of the maxilla, which encloses the roots of the teeth, marks the boundary of the palate laterally and anteriorly. Anteriorly there is a smooth transition between the palate and the alveolar process; therefore the boundary is not clearly demarcated. In the posterolateral region, however, the boundary is clearly evident since there is a sharp angle between the palate and the alveolar processes (Berkovitz et al., 2009).

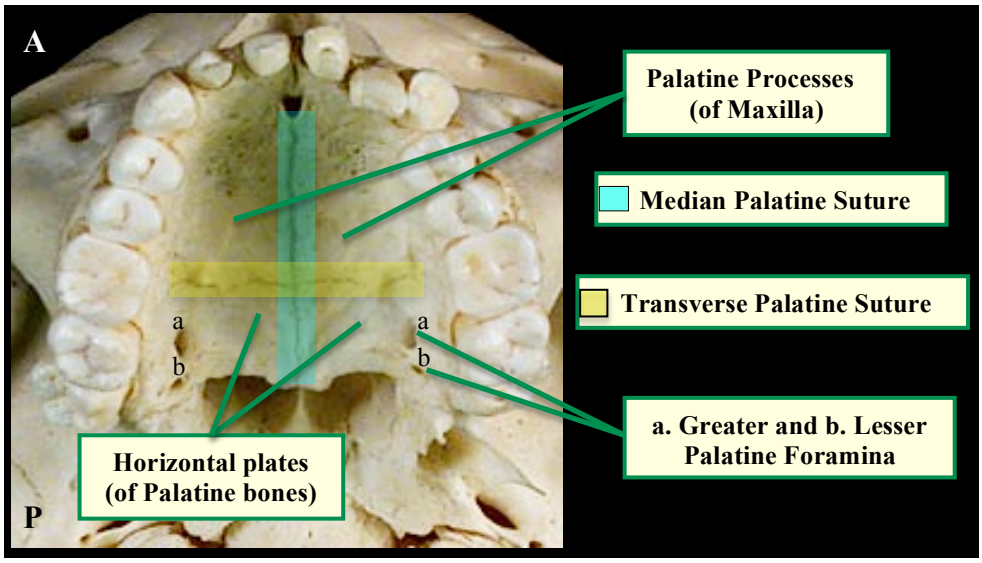

Figure 3 - Bony Composition of The Hard Palate, Inferior View*

A and P labels represent anterior and posterior

*Reprinted and modified with permission from Galil (2004), http://www.forestcity.ca/drgalil/skull/index.htm

1.1.4 Foramina, Nerves and Vessels of the Palate

The hard palate contains a few openings for the passage of blood vessels and nerves into the mucosa: the incisive foramen or fossa and the paired greater and lesser palatine foramina. The incisive foramen is an unpaired opening located at the midline, just posterior to the roots of the central incisors. It is roughly oval-shaped, and oriented in the posteroinferior direction, forming a slight depression in the anterior palate (Moore, Agur, & Dalley, 2011; Song et al., 2009). Overlying the incisive foramen is the a firm ridge of mucosa, the *incisive papilla* (Scheid & Weiss, 2012). The incisive foramen is the inferior opening of the *incisive canal* (Figure 4) a passageway containing a variable number of

small channels, providing a route for the nasopalatine nerves (from the maxillary nerve) to pass from the nasal cavities into the palatal mucosa at the incisive papilla and innervate the mucosa in this region (Scheid & Weiss, 2012; Song et al., 2009). The incisive canal also houses the terminal branches of the nasopalatine (or sphenopalatine) arteries exiting the nasal cavities to anastomose with the greater palatine artery within the incisive canal (Moore et al., 2011; Norton, 2012).

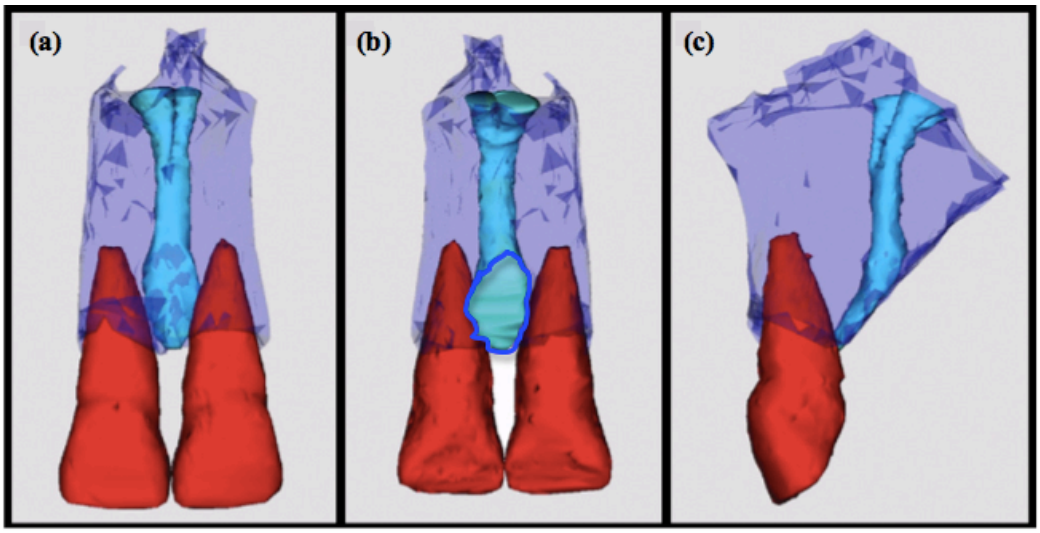

Figure 4 – Typical Incisive Canal and Foramen*

(a) Anterior view; (b) Posterior view with incisive foramen visible; (c) Lateral view
Central Incisors (red); Incisive canal (light blue); Incisive foramen (circled in blue); bone (purple-blue)

*Reprinted from Oral Surgery, Oral Medicine, Oral Pathology, Oral Radiology, and Endodontology, 108 (4), Song, Jo, Lee, Kim, Hur, HU, Kim, Shin, and Koh, Microanatomy of the incisive canal using three-dimensional reconstruction of microCT images: An ex vivo study, 583-590, 2009, with permission from Elsevier

Additionally, two paired foramina, the lesser and greater palatine foramina are present in the posterolateral hard palate for the passage of blood vessels and nerves. The bilaterally paired *greater palatine foramina* are most frequently located adjacent to the third molars (Piagkou et al., 2012), at the site where the hard palate and alveolar bone join (Figure 3). As seen in Figure 5, these foramina transmit the greater palatine nerves (originally arising from the maxillary nerve) from the nasal cavities into the mucosa overlying the hard palate. The nerves then course anteriorly along the lateral border of the palate toward the first molar, and provide mucosal innervation to each half of the palate (Scheid & Weiss,

2012). Travelling with the nerve as part of a neurovascular bundle is the *greater palatine artery*, responsible for the blood supply to the vast majority of the hard palate. The greater palatine artery travels through the pterygopalatine canal after branching from the descending palatine artery and enters the hard palate at the greater palatine foramen (Klosek & Rungruang, 2009). The lesser palatine foramina (Figure 3) are located posterior to the greater palatine foramina at the posterolateral aspect of the horizontal plates of the palatine bones (Netter, 2014). The lesser palatine foramen is most commonly singular or paired and bilaterally symmetric, however, studies have indicated the number of lesser palatine foramen can range from 1-5, albeit with decreasing frequency as the number of foramina increases (Hassanali & Mwaniki, 1984; Piagkou et al., 2012). These lesser palatine foramina convey the lesser palatine nerve and artery to the posterolateral hard palate (Moore et al., 2011) (Figure 5), where they pass posteriorly to supply the soft palate (Drake, Vogl, & Mitchell, 2015).

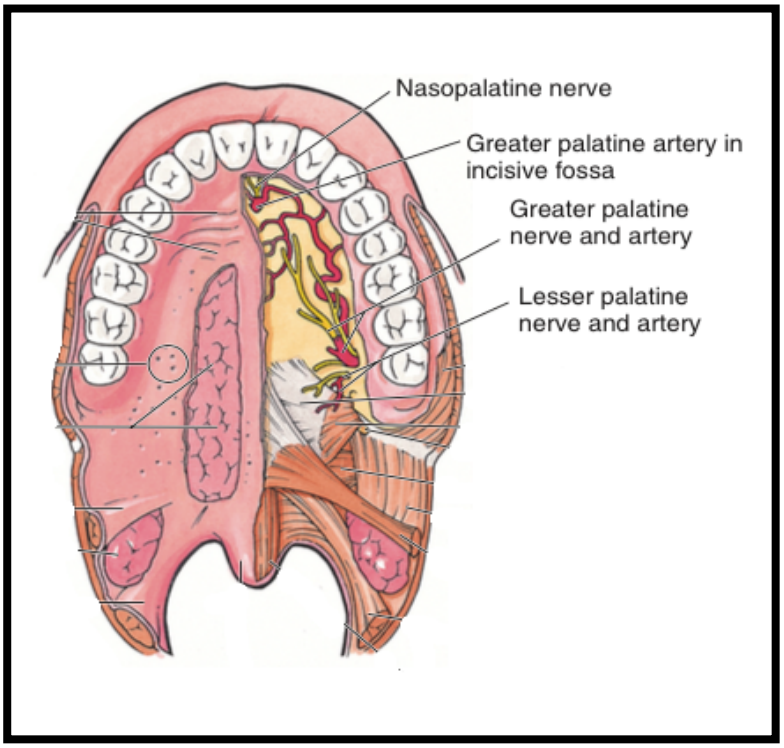

Figure 5 – Distribution of Arteries and Nerves to the Hard Palate*

*Image reprinted from Essential Clinical Anatomy, 4th Ed. By Moore, Agur, & Dalley (2010), with permission from Lippincott, Williams & Wilkins.

When considering any clinical/surgical procedures involving the hard palate, such as the placement of orthodontic miniscrews, it is apparent that care should be taken to avoid the incisive foramen (and canal), the greater and lesser palatine foramina, and their immediate surroundings along the periphery of the palate, to safeguard the neurovascular bundles and prevent incidents of severe bleeding and loss of sensation. However, because there are only a few neurovascular bundles present, none of which have major branches overlying the central bulk of the palate, the majority of the hard palate is well suited for clinical procedures such as the insertion of orthodontic miniscrews.

1.2 Orthodontic Miniscrews

As clinicians use orthodontic appliances to treat dental or skeletal malocclusions, they must also ensure there is adequate anchorage or resistance against reciprocal forces (Papadopoulos & Tarawneh, 2007). According to Newton's third law, such forces would oppose the desired direction of tooth movement (Huang, Shotwell, & Wang, 2005). Even slight reciprocal forces can bring about undesired effects, therefore the disadvantage of using teeth as anchors for the movement of others becomes obvious. In the course of orthodontic treatment, it is therefore essential that the anchor is stationary (Papadopoulos & Tarawneh, 2007). Orthodontic miniscrews are a favorable means of controlling undesired movements because they provide rigid, mechanical anchorage of intra-oral appliances to the bone (Mizrahi & Mizrahi, 2007; Papadopoulos & Tarawneh, 2007).

Orthodontic miniscrews (OMS) are small surgical bone screws composed of titanium alloy or stainless steel (Figure 6) and range in size from 5-20 mm in length and 1.0 -2.0 mm in diameter (Mizrahi & Mizrahi, 2007; Papadopoulos & Tarawneh, 2007). The terms 'implants' and 'mini-implants' generally refer to skeletal anchorage devices in which osseointegration has occurred prior to adding load, however, the term 'mini-implant' was extended in 2004 to also include miniscrews (among other terms), which by contrast do not involve osseointegration (Papadopoulos & Tarawneh, 2007). To avoid confusion with the terminology used for traditional dental implants, this thesis will use the term 'miniscrew' rather than 'mini-implant'. The present article will focus on the

bone thickness of the hard palate for the placement of such non-osseointegrated orthodontic miniscrews, which, for simplicity will be referred to as ‘miniscrews’ or ‘OMS.’

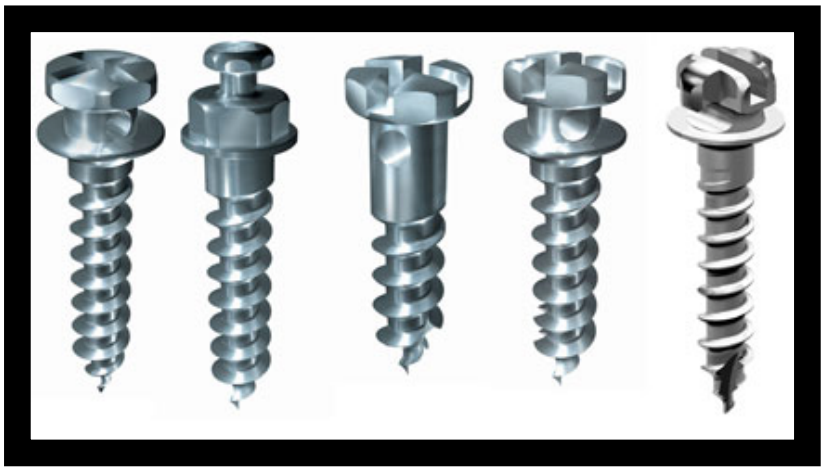

Figure 6 – Orthodontic Miniscrews of Various Designs
(Retrieved from: http://mkissdent.com/eng.php)

Recently OMSs have been used to facilitate desired orthodontic movements that were either difficult or impossible to attain using traditional orthodontic procedures (Y. H. Kim et al., 2010). Orthodontic miniscrews have been used to facilitate intrusion of molars (Chang, Y.J., Lee, H.S., Chun, 2004; Kravitz, N.D., Kusnoto, B., Tsay, T.P., hohlt, 2007), to distalize maxillary molars (S. H. Kyung, Hong, & Park, 2003) and even to distalize the entire maxillary dental arch (S-H. Kyung et al., 2009).

Orthodontic miniscrews are commonly inserted into the following intraoral bony areas: the paramedian palate, the buccal alveolar bone of the maxilla and mandible, the lingual alveolar bone of the maxilla, and the retromolar area of the mandible (Farnsworth, Rossouw, Ceen, & Buschang, 2011). Of these insertion sites, the hard palate has been widely tested and considered an acceptable site for OMSs (Gracco, Luca, Cozzani, & Siciliani, 2007; Lombardo, Gracco, Zampini, Stefanoni, & Mollica, 2010). This is namely due to the ease of accessing the palate and the minimal risk for damaging important anatomical structures, such as major blood vessels and nerves, because the vast majority of the palate’s surface is absent of large nerves and blood vessels with the exception of

the regions around the incisive foramen anteriorly (Gracco et al., 2007), and the posterolateral palate, near the greater and lesser palatine foramina (Klosek & Rungruang, 2009; Ludwig, Glasl, Kinzinger, Lietz, & Lisson, 2011) Furthermore, insertion of OMSs into the palate minimizes the occurrence of contacting and potentially damaging the roots of the teeth, an occurrence that could impede the tooth movements intended with the orthodontic treatment (Ryu et al., 2012). As previously mentioned, the hard palate is also overlaid with tough keratinized mucosa, thereby decreasing the susceptibility to inflammation, and providing additional thickness that may potentially increase the stability of the OMS (Gracco et al., 2007; Kang, Lee, Ahn, Heo, & Kim, 2007; S. H. Kyung et al., 2003).

There are however, limitations with using the palate as a site for OMS insertion. The principle concerns are a lack of bone thickness, which may lead to perforation into the nasal cavities (Henriksen, Bavitz, Kelly, & Harn, 2003) as well as high variability in bone thickness across individuals (Winsauer, Vlachojannis, Bumann, Vlachojannis, & Chrubasik, 2014). Although, the median area of the palate is seen by some as particularly favorable for OMS insertion due to sufficient cortical bone in this area (Kang et al., 2007; H-J. Kim, Yun, Park, Kim, & Park, 2006), others caution that OMS insertion is not appropriate at the median palatine suture due to incomplete calcification or fusion (Gracco et al., 2007). This is especially a concern in children and adolescents because transverse growth of the midpalatal suture progresses until the late teenage years and incomplete fusion of the suture may even persist into adulthood (Y. H. Kim et al., 2010).

Factors that influence the success of OMS include: screw diameter (Schätzle, Männchen, Zwahlen, & Lang, 2009; Wiechmann, Meyer, & Büchter, 2007), anatomical location, and the type of soft tissue at insertion site (Cheng, Tseng, Lee, & Kok, 2004), whereas sex and OMS length do not appear to be correlated with OMS outcome (Cheng et al., 2004; Papageorgiou, Zogakis, & Papadopoulous, 2012; Wiechmann et al., 2007). An important consideration when placing OMS is the amount of available bone at the insertion site, as this impacts the primary stability and therefore the survivability of an OMS (Deguchi et al., 2006; Henriksen et al., 2003; Kang et al., 2007; King, Lam, Faulkner, Heo, & Major,

2007; Stockmann et al., 2009b). Therefore it becomes obvious why accurate measurements of bone thickness would be desired.

1.3 Imaging Modalities: CT and Micro-CT

The advent of computed tomography (CT) in the 1970s revolutionized the way in which the anatomy of patients and research specimens can be visualized. Compared to the two-dimensional (2D) images captured digitally or on X-ray film, computed tomography produces three-dimensional images with increased contrast, allowing for better discrimination between tissues of comparable densities. CT also allows cross-sectional views, a feature not possible with 2D imaging techniques (Mamourian, 2013; Payne, 1978). Three-dimensional CT images are acquired by fast rotation of an X-ray tube around the patient, creating virtual 2D 'slices' in three different planes (transverse, sagittal, and coronal). Radiation detectors within the scanner sense the amount of X-rays remaining after passing through the body's various tissues (Frommer & Stabulas-Savage, 2011, Rothman, 1998, Payne, 1978,) and images are reconstructed in varying shades of gray based on the degree to which the scanned structures attenuated the X-rays. For example, the more a tissue absorbs X-rays (such that the X-rays reaching the detector have been attenuated), the brighter the X-ray image will appear. Therefore very dense structures such as bone appear white, soft tissues will appear varying shades of grey based on density, and air will appear black as it causes little X-ray attenuation (Mamourian, 2013).

Conventional CT scanners capture images using 8-10mm thick slices spaced in 10 mm intervals (Worthy, 1995; Adams, 2009). Modern high resolution CT scanners can capture 3D images with voxels around the magnitude of 1 mm^3 (Novelline, 1997; Worthy, 1995). A voxel represents a point (cube) within an evenly spaced 3D grid system, which collectively creates the image, albeit the spaces between voxels are reconstructed mathematically (Novelline, 1997). It is recognized that such scanners may have limited use with small animal imaging, given the size of voxels, therefore, higher resolution scanners would be required to adequately image smaller structures, such as those within small animals.

A newer advancement, Micro-computed tomography (micro-CT) addresses the limits of resolution seen with conventional scanners. It creates an image using the same basic principles as conventional CT but with the benefit of a smaller voxel size and, increased spatial resolution. Spatial resolution may be as high as 10μm, allowing for very detailed anatomical images (Du et al., 2007). In dental Micro-CT scanners for example, isotropic voxels can be as small as 0.136 mm, and the resulting 2D slices as thin as 1mm (Robinson, Suomalainen, & Kortesniemi, 2005). Du and colleagues (2007) stress that as Micro-CT is being used more frequently, there is a greater need for quantitative assessment of this modality.

In the case of hard palate thickness measurements obtained with micro-CT, sub-millimeter measurements would be ideal, given that the palate thins considerably at the posterior region, with less than a millimeter of bone thickness expected. As we approach the limits of resolution, however, we question whether the micro-CT image of bone preserves its detail or whether thin areas become progressively fuzzy, thereby causing an observer to potentially misjudge the absolute surface of the bone.

1.4 Literature of Interest

Of the numerous studies assessing palatal bone thickness to date, there still exists limited literature on cadaveric studies of palatal thickness. An assessment of the available literature focusing on hard palate bone thickness revealed a predominance of in-vivo studies, largely encompassing orthodontic patients and predominantly using cone beam computed tomography (CBCT) imaging. Similar to in-vivo studies, Baumgaertel (2009) measured palatal bone thickness in human cadavers using CBCT, however, six additional cadaveric studies identified in a 2012 review by Winsauer and colleagues, have relied on examination by cephalometric radiographs (Henriksen et al., 2003; Jung, Wehrbein, Heuser, & Kunkel, 2011a; Wehrbein, Merz, & Diedrich, 1999) or histological examination (Stockmann et al., 2009b; Wehrbein, 2008, 2009b). Cephalometric radiographs, however, may underestimate true bone thickness (Crismani, Bertl, Celar, Bantleon, & Burstone, 2010; Wehrbein et al., 1999) and their use should be limited to assessments of the paramedian palate only (Bourassa, 2015). Histologically, BT can be

assessed and may be visually separated out in terms of bone type (i.e. cortical vs. trabecular bone thickness) (Ross & Pawlina, 2011), however this method is limited two dimensional analysis and is very time consuming/ labor intensive, given its reliance on chemically processing and serially sectioning the bone in order to obtain measurements (Buchman, Sherick, Goulet, & Goldstein, 1998; Gielkens et al., 2008; Jiang et al., 2005).

To the best of my knowledge, no studies to date have focused on traditional gross anatomical (physical) measurements of hard palate thickness. Thus the current study aims to address this gap in the literature. The only study, thus far to closely resemble gross anatomical sectioning methods was a histological study carried out in 2006 by H-J. Kim and colleagues in which they decalcified and sectioned the bone to investigate both cortical bone and soft tissue thickness. Given that the protocol relied on decalcification of the bone, this technique could potentially compromise accurate measures of the true thickness, since bone contains a large proportion of calcium phosphate, stored in the bone as hydroxyapatite crystals (Ross & Pawlina, 2011). In contrast to such histological methods, micro-CT is less destructive to the tissue, typically acquires a larger number of slices and allows visualization in three dimensions, thereby permitting more comprehensive analyses (Buchman et al., 1998; Jiang et al., 2005). It is highly correlated to histological examination of bone (Gielkens et al., 2008; Kuhn, Goldstein, Feldkamp, Goulet, & Jesion, 1990).

The use of micro-CT in the assessment of the hard palate is very scant in the literature, however. Because the accuracy of a micro-CT system is dictated by the x-ray dose, this high-resolution imaging technique therefore relies on a high radiation dose (Kiessling, Pichler, & Hauff, 2010). This obviates its impracticality for in-vivo human research and is the likely reason its use in imaging the human palate is underreported in the literature. Micro-CT has been typically used in live, small animal imaging or in-vitro studies (Holdsworth & Thornton, 2002; Kalender, Deak, & Engelke, 2011) and has been predominantly utilized for non-invasive assessment of trabecular bone (Feldkamp, Goldstein, Parfitt, Jesion, & Kleerekoper, 1989; Guldberg et al., 2003; Kuhn et al., 1990). Micro-CT is superior to histological examination in terms of the efficiency with which images are acquired (Guldberg et al., 2003). It can be used to separately assess the

thickness of trabecular and cortical bone (Bagi et al., 2006; Feldkamp et al., 1989) and can be used to determine bone mineral density (Ito, 2005; Prevrhal, 2005) should further analysis of bone quantity be desired. For example, this would be useful information to include in research aimed to guide clinicians' placement of OMS, such as when carrying out a comprehensive anatomical mapping of the hard palate. Given its high spatial resolution and ability to assess the tiny microarchitecture of bone, it was hoped that this would provide an accurate representation of the hard palate.

1.5 Purpose of Study

The present study attempts to validate whether micro-CT is a suitable tool for the assessment of hard palate bone thickness. Specifically, the research question posed is: do micro-CT measurements of hard palate bone thickness agree with physical 'gold standard' measurements obtained through gross anatomical dissection. The motive for the current study is the need for a comprehensive anatomical mapping of hard palate thickness, which can be efficiently obtained with a large sample size, in order to better inform clinicians which regions of the palate most commonly possess sufficient bone to engage an orthodontic miniscrew.

By supplementing the micro-CT data with anatomical measurements of the palate, this study attempts to fill the need in the literature for additional cadaveric studies assessing the hard palate by gross anatomical dissection. By characterizing the thickness of the palate at numerous sites, it is also hoped that the study will complement current literature in terms of general bone thickness trends seen in the palate and establishing which sites of the hard palate provide adequate bone thickness for safe OMS placement.

1.6 Hypothesis

It is hypothesized that no significant differences will exist between bone thickness measurements obtained by Micro-CT and gross anatomical dissection; Micro-CT is hypothesized to be adequate tool for the assessment of hard palate bone thickness.

2 Materials and Methods

2.1 Specimen Selection and Exclusion Criteria

The heads of fourteen embalmed human cadavers were obtained from Western University's gross anatomy lab. All cadaveric subjects were obtained with permission from the body bequeathal program at Western University, London ON, Canada in accordance with the Anatomy Act of Ontario and Western's Committee for Cadaveric Use in Research. The University of Western Ontario embalming fluid contains ethanol, propylene glycol, methanol, phenol and formaldehyde. Given that this study shared the same set of specimens with a concurrent study by Bourassa (2015) subject inclusion criteria, therefore follows the protocol established by Bourassa including: intact hard palate, presence of at least four anterior teeth, absence of gross anatomical abnormalities (such as torus palatinus) or bony pathologies (such as osteoporosis). Some of the subjects were previously dissected for educational purposes but without compromise to the maxilla. Ideally, subjects with full dentition were desired, however, given the advanced age of the donors, and a limited number of donors with intact maxilla this was not feasible. As stressed by Bourassa (2015), the presence of anterior teeth is essential for the concurrent study and therefore the present study as well, to ensure comparable location of the incisive foramen across specimens. This decision was based on the findings of Song and colleagues (2009) who established that incisive foramen in edentulous subjects lies slightly more anterior than its location in dentate subjects. Therefore, by selecting subjects with anterior teeth, it was expected that the position of the incisive foramen would not be impacted.

After eliminating subjects based on the exclusion criteria, ten subjects (7 males, 3 females) were selected for measurement purposes. The subjects' ages ranged from 54-98, with a mean age of 77.6 years. Equal proportions of the sexes were not feasible because additional female donors did meet the inclusion criteria (e.g. had maxillary tori, were edentulous, or had significant bone resorption). This unequal proportion of the sexes was deemed acceptable, however, given the objective of the study was not to determine how

BT trends relate to subject demographics but rather to assess whether micro-CT is an accurate tool for measuring palatal BT.

2.2 Maxilla Isolation, Preparation and Storage

To facilitate removal of the maxilla, the soft tissue of the face, overlying the maxilla, was partially removed using basic dissection tools (scalpel, rat tooth forceps, scissors, and periosteal elevator). The maxilla was then removed through a series of cuts using a BIRO band saw (model no. 22, Marblehead Ohio, USA3) designed for meat and bone and the mandible was physically disarticulated from the maxilla at the temporomandibular joint (TMJ). A horizontal cut was made through the cranium approximately 1 cm above the inferior margin of the orbit (Figure 7a). Vertical cuts were made lateral to the dental arch on the left and right side of the cranium at the region where the zygomatic processes of the maxilla join with the zygomatic bones (Figure 7b). A final vertical cut was made posterior to the maxillary tuberosities, removing all bone posterior to the nasal cavities, (Figure 7c) thereby freeing the specimen from the rest of the cranium. An isolated specimen, following further dissection, can be seen in Figure 8.

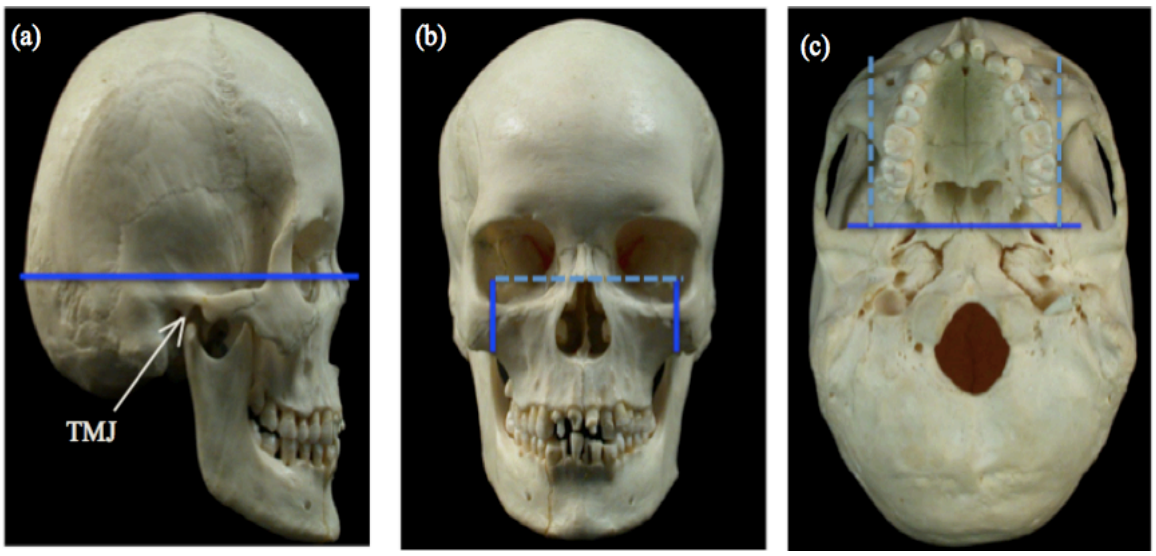

Figure 7- Location of band saw cuts for palate isolation*

(a) Horizontal cut approximately 1 cm superior to orbital floor;
(b) Vertical cuts lateral to dental arch (solid lines);
(c) Vertical cut (solid line) posterior to maxillary tuberosities (arrowheads)

* Reprinted and modified with permission from Galil (2004), http://www.forestcity.ca/drgalil/skull/index.htm

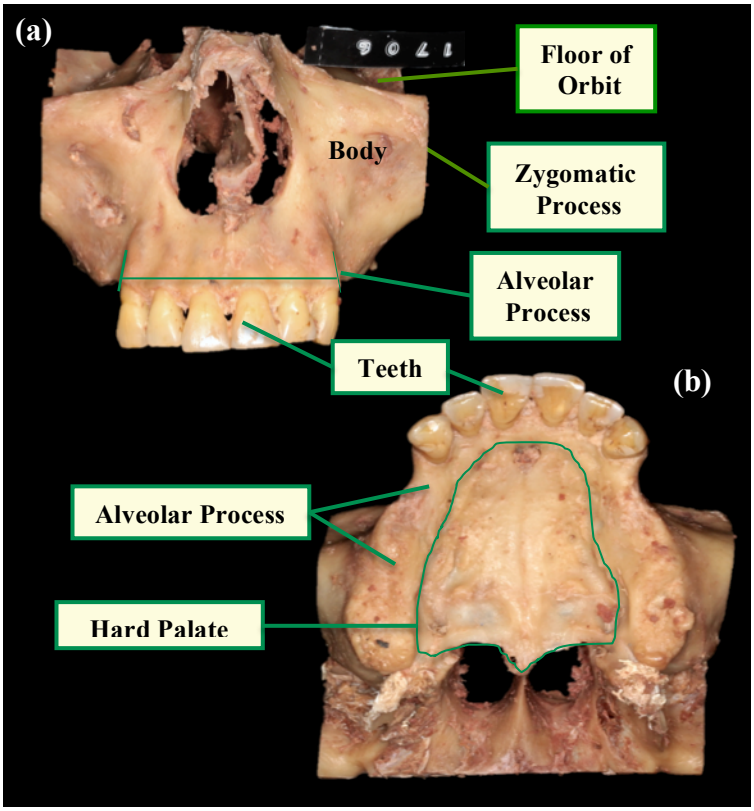

Figure 8 – Isolated Maxilla Following Gross Anatomical Dissection*

(a) Anterior view; (b) Inferior View

Using the same dissection tools, isolated maxillae were stripped of remaining soft tissue including gingiva, palatal and nasal mucosa, and periosteum. Care was taken around the posterior palate to avoid damage to the bone as numerous studies indicate the bone is very thin in this region (Baumgaertel, 2009; Farnsworth et al., 2011; Gracco et al., 2007; Kang et al., 2007; Ryu et al., 2012).

To prevent image artifacts during micro-CT scanning the anatomical crowns of the teeth with metal-containing dental restorative materials (e.g. crowns or fillings) were sectioned using a *Stryker* bone saw (model no. 810, *Mopec,* Oak Park, MI, USA). To ensure all specimens were treated with the same protocol, all of the crowns were removed, including those not containing dental restorative materials.

During initial isolation of the maxilla, most of the bone forming the nasal cavities was retained to provide sufficient anchorage of each specimen within an acrylic block while

maintaining at least 1 cm of clearance between the superior surface of the palate/ nasal floor and the acrylic for ease of subsequent palate isolation. Specimens were embedded in acrylic which entailed adhering the inverted specimens to the bottom of a square plastic container (mold), roughly leveling the palate using boxing wax strips (*KaVo- Kerr*™, Orange, CA, USA), and pouring self-cure Orthodontic Resin (*Dentsply Caulk,* Woodbridge, ON, CAN) into the mold. This resulted in an acrylic block of consistent length and width for each specimen. Specimens were embedded with the nasal cavities partially in the acrylic and the hard palate facing superiorly (Figure 9). The acrylic block served as a rigid base to secure specimens during OMS insertion in the concurrent study by Bourassa (2015), and for the purpose of both studies, the acrylic block served as a means to ensure specimens were placed in the same orientation for Micro-CT scanning as the block was outlined on the scanning platform.

To prevent desiccation of the specimens and inhibit bacterial growth following isolation and dissection, each specimen was wrapped in cotton or linen cloths soaked in 1% Dettol (an antiseptic wetting solution) and placed in plastic bags within a sealed container. This procedure was followed prior to and following embedding in acrylic.

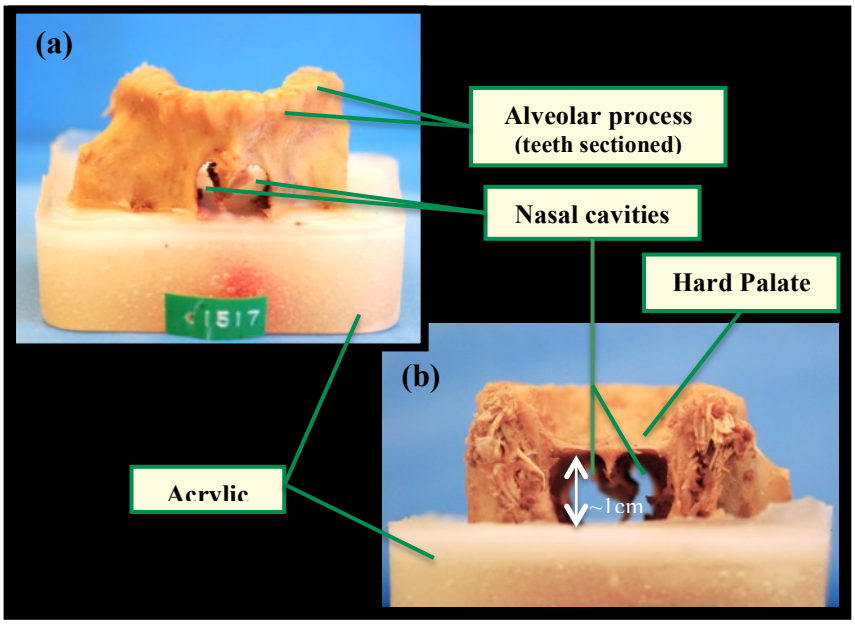

Figure 9 - Specimen embedded in Acrylic Following Teeth Removal
(a) Anterior view; (b) Posterior view

2.3 Selection of Measurements Sites

Initial selection of measurement sites was carried out by Bourassa (2015) following a thorough literature review. Thirteen sites were chosen, representing the majority of the hard palate. These sites included those most commonly reported in the literature for OMS placement in the palate as well as sites at which OMS insertion could be inserted based on lack of contact with important anatomical structures. Points were spaced 4 mm apart in the medial to lateral direction, beginning 2 mm lateral to the median palatine suture and extending out 10 mm lateral to the suture. Points were spaced 6 mm apart in the anterior to posterior direction, beginning 3 mm posterior to the incisive foramen For simplicity, Bourassa (2015) renamed the sites using a 1-5 numbering system and the terms parasagittal (P), sagittal (S) and lateral (L) based on anatomical location from the median palatine suture. This was adopted for the current study as well and can be seen in red text in Figure 10. For a thorough review sites and the anatomical/ dental landmarks (teeth) to which they correspond, see Bourassa (2015).

For the current study, gross anatomical measurements were carried out following micro-CT scanning and miniscrew removal by Dr. Bourassa. Therefore, it was the intention that all 13 sites would be included for anatomical comparison provided that: (1) the bone surrounding the OMS hole remained intact, and (2) the terminus of the hole could be accessed without the need for further dissection, aside from extension by a longer OMS. At sites where the BT exceeded the length of the 6mm OMS inserted by Dr. Bourassa, the holes were extended using a longer VectorTAS^{TM} OMS (12 mm in length by 2.0 mm diameter, manufactured by Ormco^{TM}, Orange CA, USA). Extension of holes was typically required at anterior sites PS1, S1, and L2. Sites extended (by specimen) can be found in Appendix D. If the 12 mm screws resulted in a visible perforation through the bone, the sites were included for measurement. Sites at which the 12 mm screws terminated within the air filled space enclosed by the alveolar process were excluded from measurement. This exclusion was decided on the basis that additional dissection using the bone saw would potentially introduce measurement errors if a small fraction of the hard palate was damaged in the process.

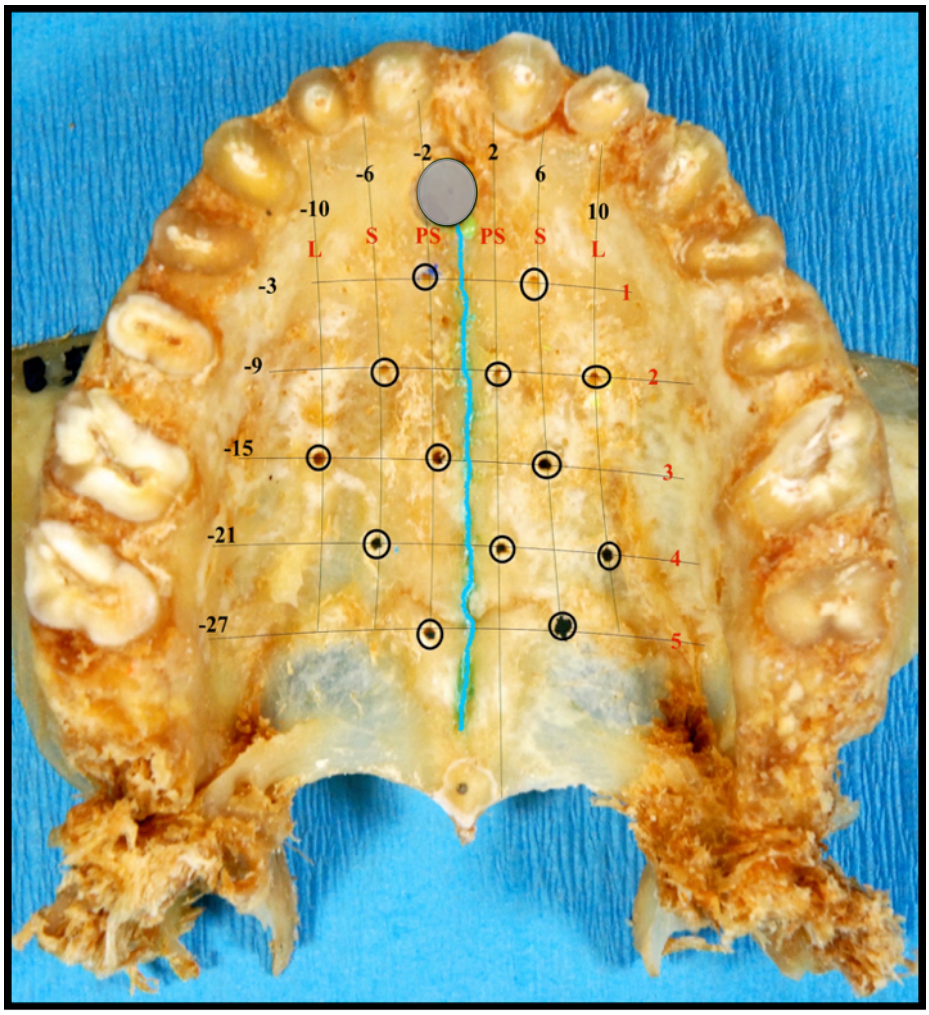

Figure 10 – Specimen Following OMS Insertion Indicating BT Measurement Sites

Black circles denote location of measurements site (OMS holes); grey circle indicates incisive foramen; **L**, **S**, and **PS** represent lateral, sagittal, and parasagittal locations, respectively

2.4 Micro-CT Imaging and Bone Thickness Analysis

Specimens were imaged using micro-CT at Robarts Research Institute, Western University. Scanning was carried out using the GE eXplore Ultra, a volumetric cone beam Micro-CT scanner, (*GE Healthcare*, London, ON, CAN) seen in Figure 11, with a spatial resolution of 0.18mm and an isotropic voxel size of 0.15 mm. The x-ray source and flat panel detector lie opposite on another in the gantry, which moves around the

specimen (Du et al., 2007), thus this scan is of the rotating variety, typically used for live animal imaging, in which the specimen remains stationary (Robinson et al., 2005). During 16 second scan acquisitions, the detector obtained 1000 projection images with a matrix size of 1024 x 680. From these 2D images, a 3D image (volume) was reconstructed using the technique of back projection, resulting in a 3D image that is 1024 x 1024 x 680 voxels (Bourassa, 2015).

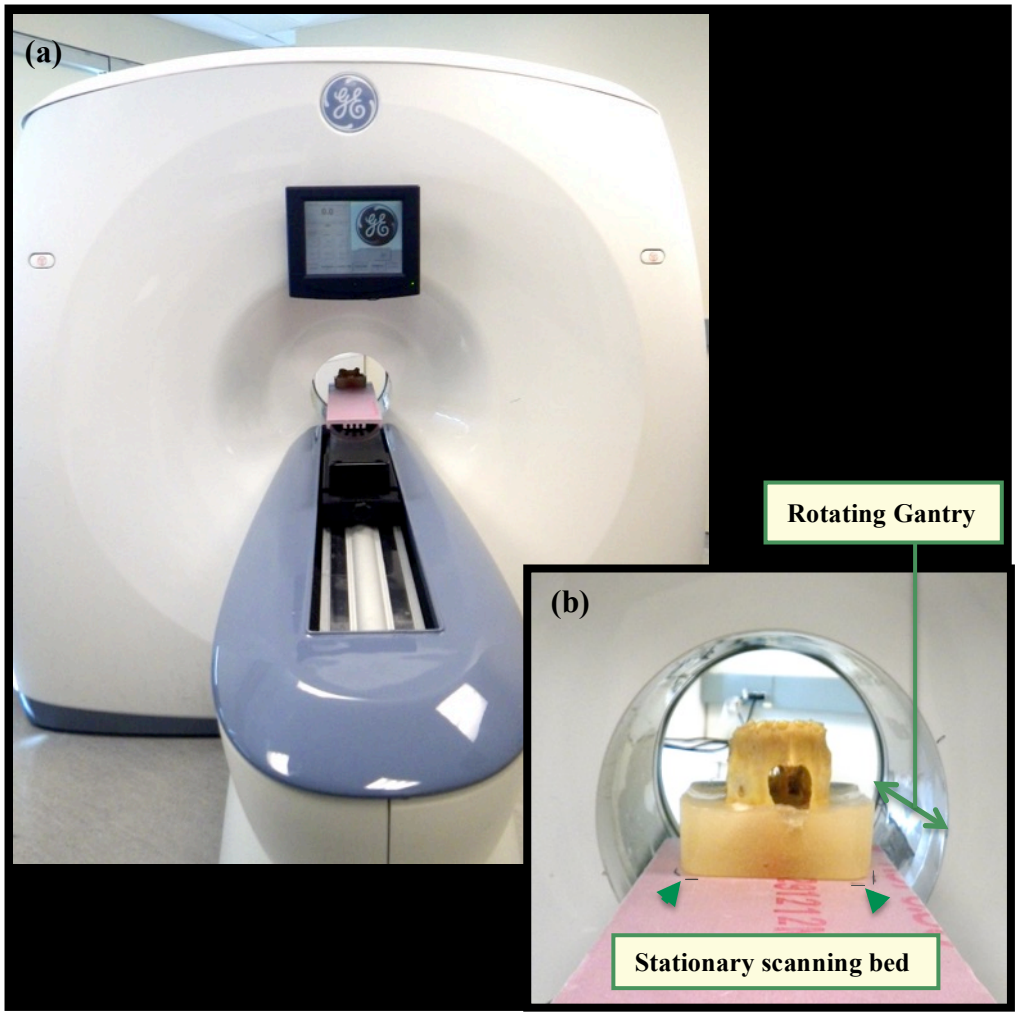

Figure 11 - Micro CT Scanning of Specimens, Robarts Research Institute

(a) GE eXplore Ultra Micro CT scanner; (b) Position of specimen on scanning bed; arrowheads indicate marking of specimen location on scanning bed

Measurements of Micro-CT bone thickness (BT) were obtained with permission from Bourassa (2015). These values were calculated by Dr. Bourassa using greyscale graphs in Hounsfield units (HU), which represented the longitudinal trajectory of an OMS through the bone at each site of interest (see Bourassa (2015) for detailed protocol).

2.5 Gross Anatomical Measurements and Validation

Gross anatomical measurements (referred to subsequently as "physical measurements" for brevity) were taken at the same sites assessed for thickness by Bourassa (2015) using micro-CT. Physical measurements were taken following OMS removal by Bourassa (2015), which resulted in approximately 1.3 mm diameter holes in the bone at each of the 13 sites of interest. A method was devised to measure palatal BT at these sites. Since the micro-CT thickness measurements of the palatal bone at the OMS sites were already reported by Bourassa (2015), direct comparisons with physical measurements of BT could be used to determine the agreement of these measures.

2.5.1 Measurements Validation

Prior to taking physical measurements, a pilot study was carried out to ensure the physical measurement technique (a hole depth measurement) was valid. Five cedar wedges were created to simulate the general structure of a sagittal section of the palate, having an anterior curvature and thinning from anterior to posterior. The superior surface of the wood represented the palatal surface. Wood was chosen because of its ability to be easily shaped, especially thinly, and because it could handle miniscrew insertion without significant compression near the screw head or fracture at relatively thin areas (compared to the other materials tested: dental stone, rubber piping, paraffin wax, and compressed Styrofoam).

Thickness measurements were obtained by digital caliper at six evenly spaced sites marked as dots along the cedar wedges. To standardize caliper measurements, the following lines were drawn to align the caliper jaws for each measurement: a horizontal line through the center of each site (1-6), perpendicular to the lateral edged of the wood, and a vertical line, on the left and right sides of the wedge. Vertical lines began at each end of the horizontal line and were oriented perpendicular to the superior surface of the

wood to represent the trajectory of a miniscrew through the wood (Figure 12). For each measurement, the jaws of the digital caliper were lined up with the vertical and horizontal lines, while ensuring one tip of the caliper jaw coincided with the center of the measurement point (Figure 13). To account for potential differences in thickness from left to right, measurements were taken with the caliper oriented on the right side of the wedge (lined up with the right vertical reference line) and again with it oriented on the left side of the wedge (lined up with the left vertical line). Values from the left and right side were averaged to approximate a measurement of thickness directly at the centrally located points. Measurements were taken three times for each site and the average values were reported. See Appendix E for the averaged data.

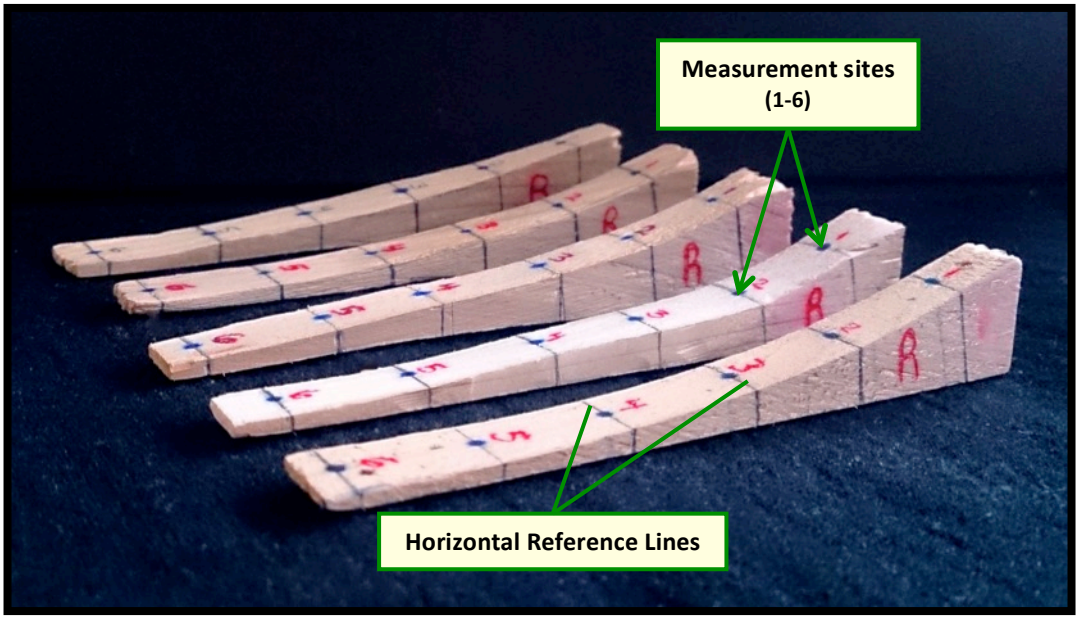

Figure 12 - Cedar Wedges Used for Measurement Validation

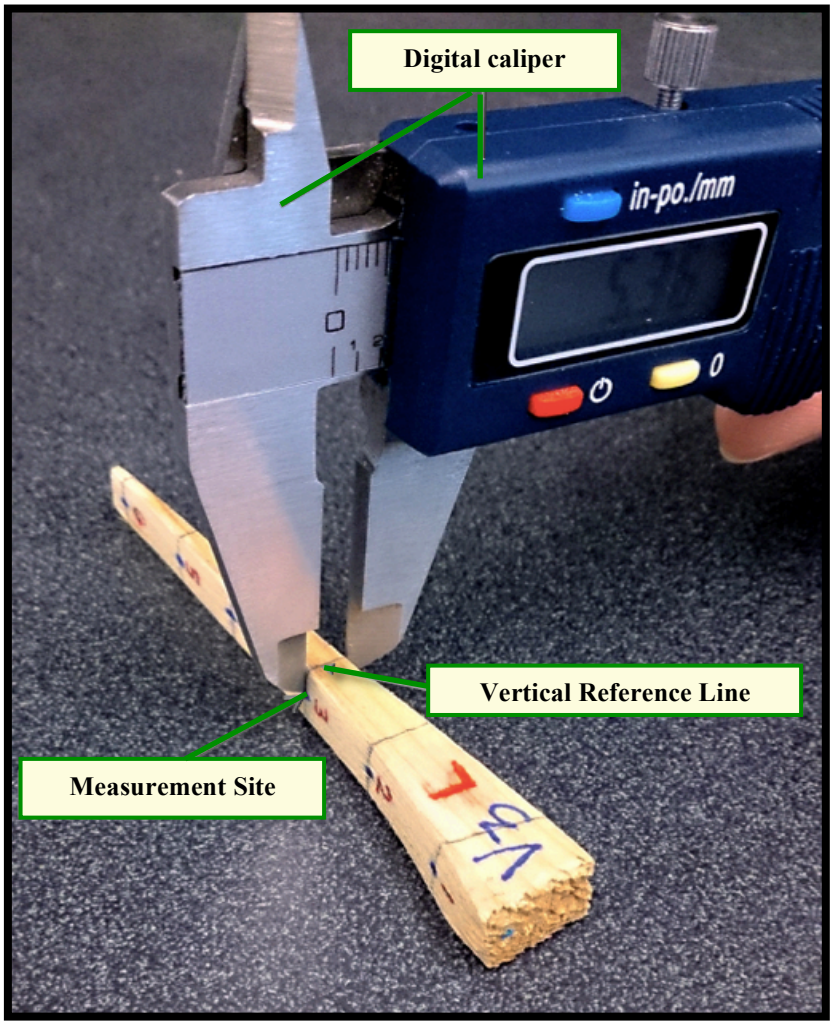

Figure 13 – 'Gold Standard' Caliper Measurements Used for Measurement Validation

To prepare the cedar wedges for hole-depth measurements of thickness, self-drilling VectorTAS™ orthodontic miniscrews (Ormco™, Orange, CA, USA) were inserted perpendicular to the superior surface of the wood and subsequently removed at each of the six sites (Figure 14), creating holes approximately 1.3 mm in diameter and up to 6mm in length. For the thicker anterior 1-2 sites in which the 6 mm length screws did not perforate completely through to the inferior side, longer screws of the same type (12 mm length by 2 mm diameter) were used to perforate the thicker wood, resulting in a 2 mm diameter hole. Holes were sealed off at the inferior end by applying squares of hockey tape (Renfrew™, *Scapa*, Renfrew, ON, CAN), to the undersurface of the wood. This was

reinforced by a second layer of tape, following by dripping melted inlay casting wax (Kerr™, Orange, CA, USA) onto the taped surface to provide rigidity at the terminus of the hole.

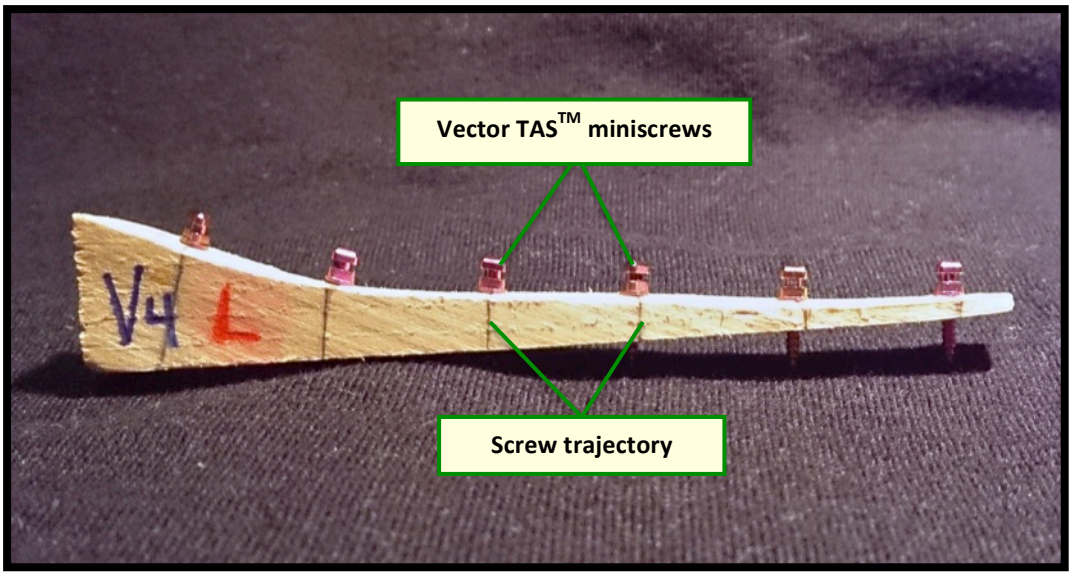

Figure 14 - Insertion of Orthodontic Miniscrews into Cedar Wedge
Horizontal reference lines represent the trajectory of the screw 90° to the wood surface

Physical measurements were taken at each of the OMS holes with the aid of a stainless steel dissection pin obtained from the Western University gross anatomy lab. The pin was intentionally dulled at the tip, and gently passed into the OMS holes at the superior surface of the cedar wedge until resistance from the hockey-tape/casting wax was felt at the inferior surface. Using fast drying, red blocking ink (*Speedball*®, Statesville, NC, USA) and a fine art brush (Micron, Bent liner #15/0, *Dynasty*®, Glendale, NY, USA) with a 1mm brush width, a fine line was marked on the dissection pin at the superior surface of the wood (Figure 15). The distance from pin tip to the red ink line represents total thickness. The pin was measured from tip to ink line using a digital caliper (*Mastercraft*®, Canadian Tire). To accurately measure the distance from pin tip to ink line, a surgical/ dissecting microscope, equipped with a USB microscope digital camera (*OMAX*, model no. A3530U) was used to magnify and view the pin and caliper on a

laptop monitor. To standardize physical measurements, the caliper was fixed to a board in the horizontal plane, the same pin was used for all measurements, and a magnet was fixed under the caliper jaws to minimize movements of the pin during measurements (Figure 16). Measurements were taken three times (immediately following one another) for each marked pin and the averaged values were reported. A second set of measurements was taken following the above protocol, following an interval of at least one day, to allow for averaging of data to minimize potential human error associated with the measurements. Averaged values can be viewed in Appendix E.

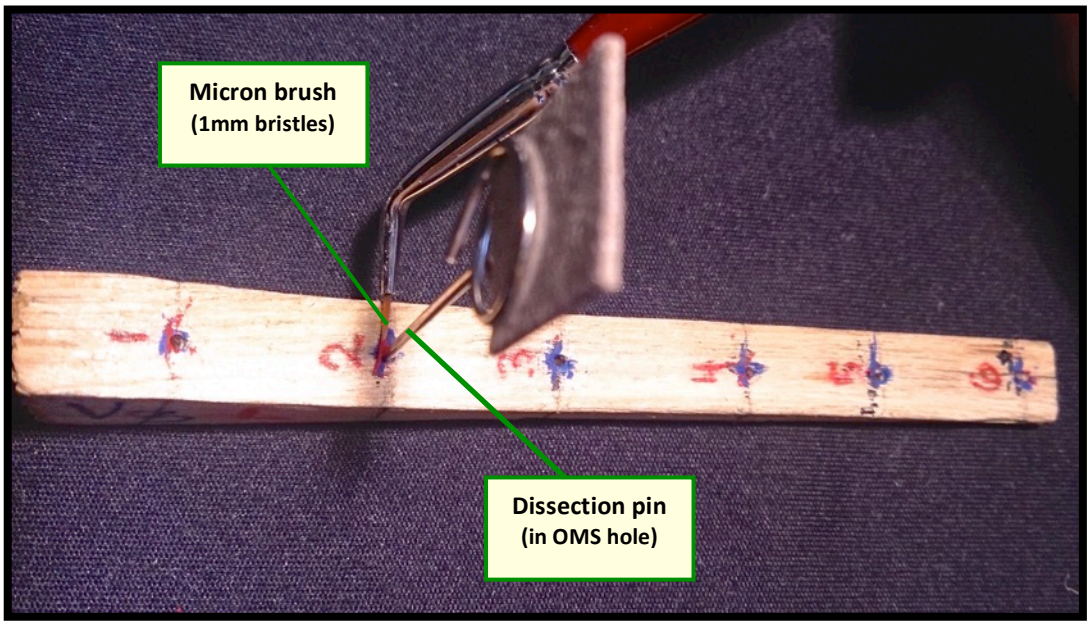

Figure 15 - Marking of Dissection Pin for Depth Measurement

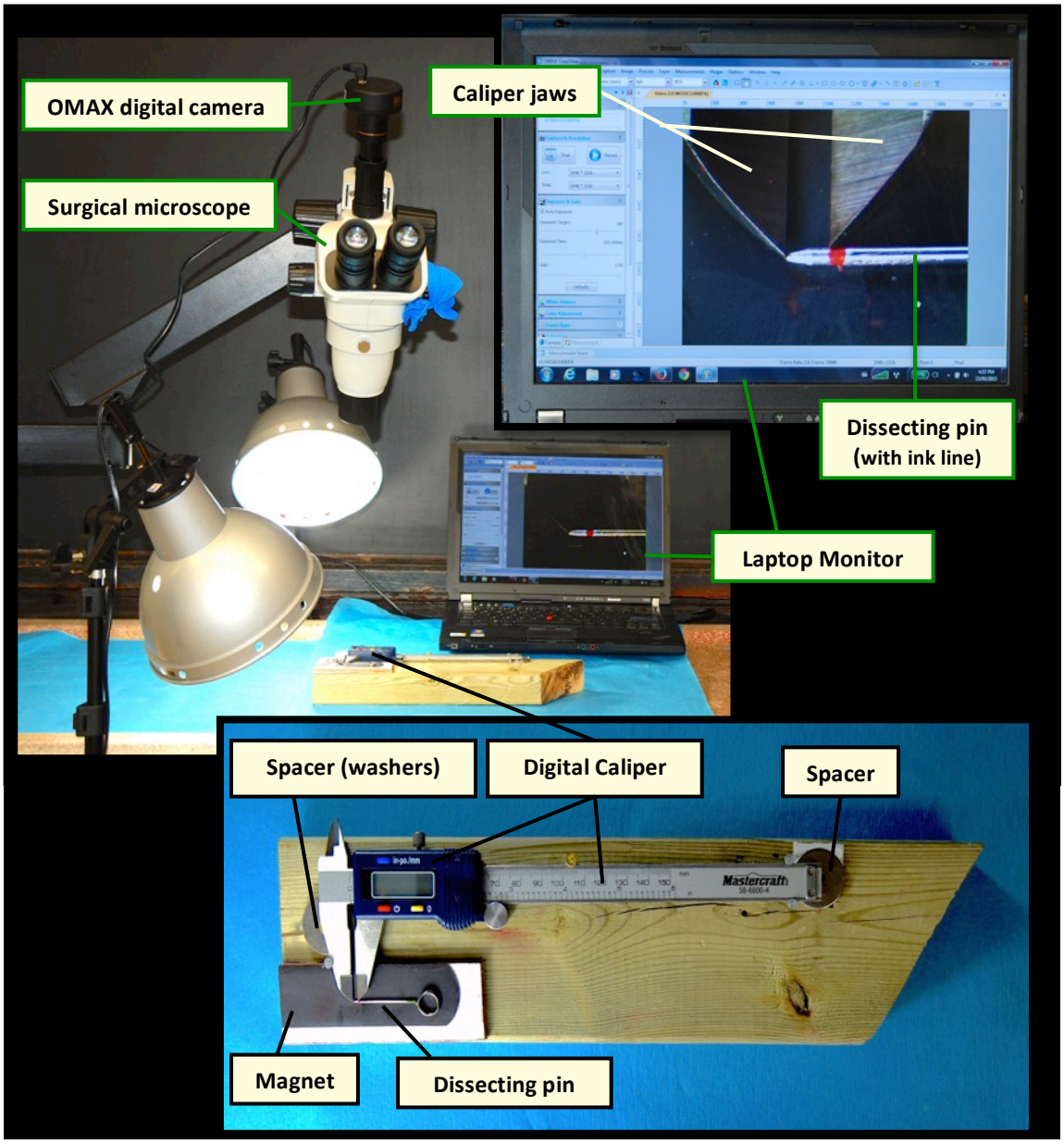

Figure 16 – Setup and Standardization for Anatomical Measurements

2.5.2 Gross Anatomical Measurements

In preparation for physical measurements, the palate was isolated from the acrylic block using the BIRO band saw (Figure 17). Following the same protocol as the pilot (validation) study, each OMS hole was sealed off at the terminal end in the nasal cavities using individual squares of water-resistant hockey tape. This was followed by a second

layer of tape to prevent potential seepage of materials into the holes. Melted casting wax was dripped into the sealed-off nasal cavities to provide rigid structure at the terminus of the OMS holes and therefore denote the termination of the bone at the nasal surface (Figure 18).

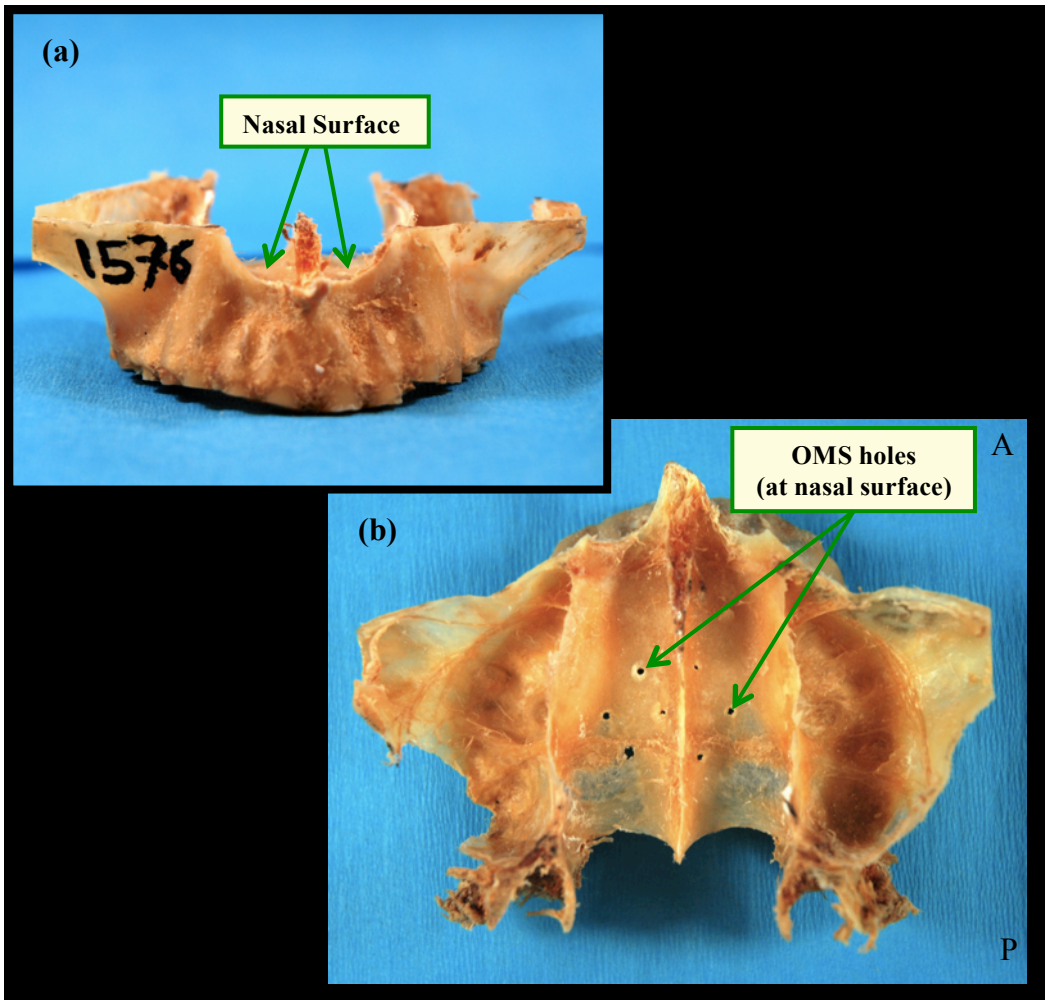

Figure 17 - Isolated Specimen Following Acrylic Removal

(a) Anterior View; (b) Superior View

A – P labels indicate anterior and posterior

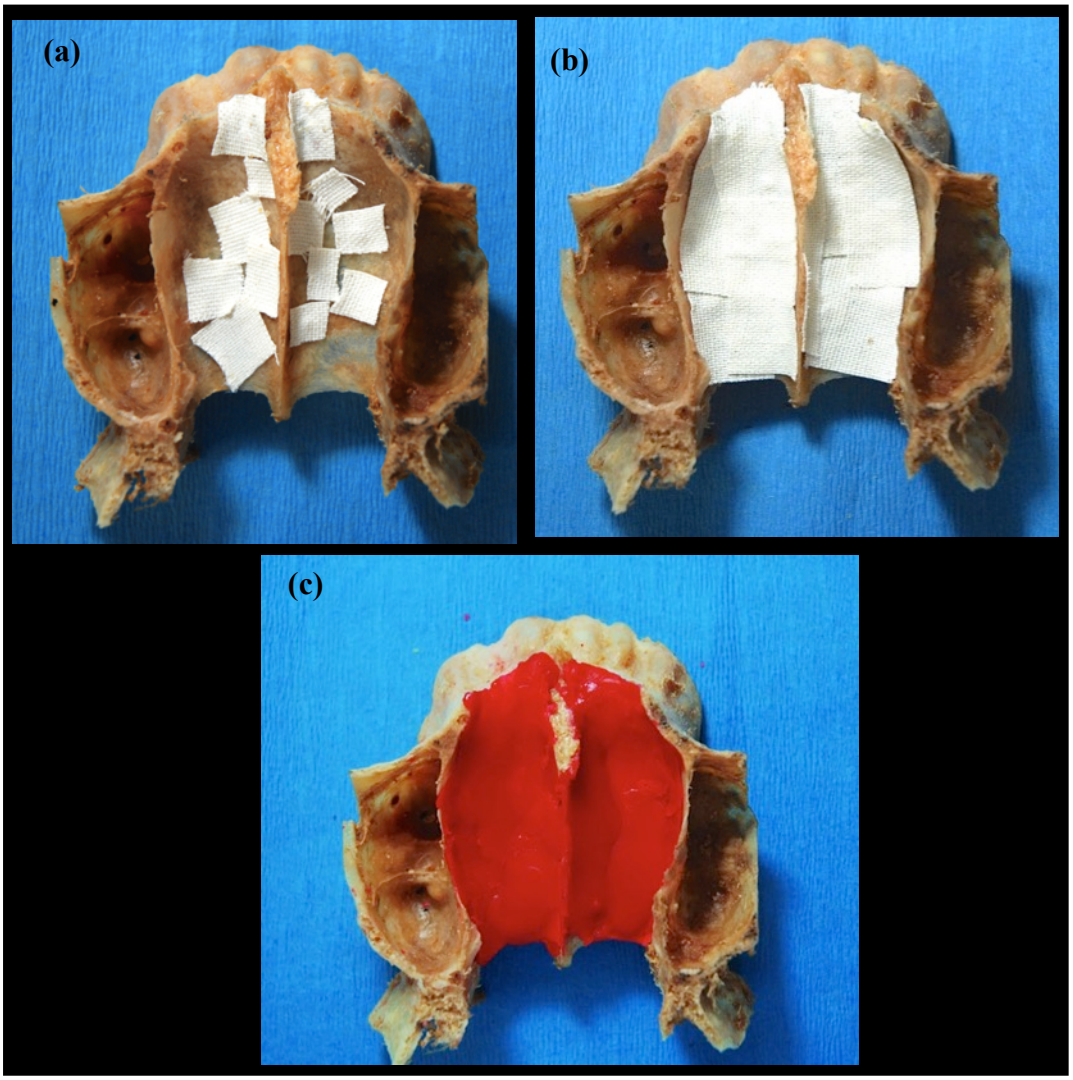

Figure 18 – Preparation of Specimen for Physical Measurements, Superior View

(a) Hockey tape sealing individual OMS holes at nasal surface
(b) Nasal cavities sealed off with hockey tape
(c) Nasal cavities filled with inlay casting wax (red)

A stainless steel dissection pin, intentionally dulled at the tip, was gently passed into the OMS holes at the oral surface of the hard palate until resistance from the hockey-tape/casting wax combination was felt. Using red blocking ink and a very similar fine art brush (bristles = 1mm thickness), a line was marked on the dissection pin at the palatal surface of the bone. The distance from the tip of the pin to the ink line represents palatal BT (mm) and was measured with digital caliper, using the same setup as the pilot study

(fixed caliper view under surgical microscope). Measurements were taken three times for each marking of the pin and averaged values were reported. A second set of measurements was repeated at a later date with a least a two-day interval between the same specimens. A second independent rater took a third set of physical measurements using the same protocol.

2.6 Statistical and Graphical Analysis

Prior to analysis of gross anatomical and Micro-CT data, measurements from the pilot study were analyzed to determine whether the physical measurement technique was valid. Digital caliper measurements (considered our gold standard for measurement in the anatomy lab at Western University) were compared to pin measurements on the basis of percent error. The criterion set for determining the validity of the measurement technique was a maximum average of 5% error and high repeatability of measurements (> 90%). If the average error fell above this cut-off value, and/ or repeatability between measurements was low, the pre-determined decision was to render the measurement technique unacceptable. Percent error was calculated using the following equation, using caliper measurements as the gold standard (actual) values and the pin measurements as the experimental values: **Percent error = | [(experimental-actual)/actual]*100 |.**

Using the software SPSS®, version 22.0 (IBM® Corporation, Armonk, NY, USA) descriptive statistics including mean, median, and standard deviation, were determined for measurements differences. Inferential statistical tests, discussed below, were run to analyze the differences between the palatal BT measurement techniques.

Two-way mixed, Intraclass Correlations (ICC) were determined to assess the absolute agreement between gross anatomical measurements taken by rater one (inter-rater reliability) and between the averaged measurements reported by rater one to measurements taken by rater two (intra-rater reliability). High intra-rater and inter-rater reliabilities (> 90%) were desired, to ensure both raters had stringently followed the measurement protocol.

To determine whether significant differences exist between the measurement techniques (on a site-by-site basis), the difference between BT measurements obtained from micro-CT and physical measurements was calculated (mm), and the distribution of the differences at each palatal measurement (e.g. PS1, L2, etc.) was assessed for normality using the Shapiro-Wilk test ($\alpha = 0.05$). The Shapiro-Wilk test indicated that approximately half (7) of the palatal measurement sites displayed a normal distribution of measurement differences ($p > 0.05$), whereas the other half of the sites (6) violated the assumption of normality ($p < 0.05$), and thus, based on this violation, non-parametric tests were chosen to statistically analyze the relationship and agreement between gross anatomical (physical) measurements and Micro-CT measurements of hard palate BT.

Two-tailed Spearman's rank correlations (r_s) were carried out to determine the potential existence and strength of a relationship between physical and Micro-CT measurements of BT. However, because some studies have indicated that Pearson's correlation is relatively insensitive to non-normality (Edgell & Noon, 1984), and because this statistical test is more commonly used and therefore more familiar to most (McDonald, 2014), a Pearson's correlation (r) was also reported to illustrate the linear relationship between the two measurements, and its strength. Correlation, however, is limited in its descriptiveness since it only indicates the strength and direction of a relationship but does not indicate whether there is absolute agreement between the measurement techniques (Bland & Altman, 1986).

Given the limitations of correlations, Bland-Altman plots were created to better illustrate the relationship between Micro-CT and physical measurements of hard palate BT in terms of agreement. These plots compare the differences between measurements from two modalities against the means of the two measurements. If assessments from one tool/technique adequately agree with those from another (according to one's predetermined clinical definition of agreement), the tools techniques can be used interchangeably (Bland & Altman, 1986, 1999; IBM, 2012).

Taking into account that human error would play a role in measurement taking, we defined sufficient agreement as measurement differences up to but no larger than 10% of

the average value of the two measurements. For example, this equates to an allowable discrepancy of 0.05 mm between modalities for thickness measurements of 0.5 mm and a 1.2 mm discrepancy for physical measurements of 12 mm. This allows for a greater margin of error in terms of thickness in regions where there is more bone in the first place and therefore less risk of sinus perforation from OMS as documented by Bourassa (2015). Based on our modified definition of agreement, and the assumption that if measurements closely agreed, the average difference between them would be close to zero, our limits of agreement were plotted as reference beginning from the origin using the following equations: $y = + 0.1x$ (upper limit) and $y = - 0.1x$ (lower limit).

After comparing the difference as a whole, the Kruskall Wallis H test was performed ($\alpha = 0.05$) to determine whether there are significant differences in measurement difference (micro-CT – Physical measurement (mm) based on site (e.g. L1, PS1 etc.). Essentially we are asking: does the difference between the two measurement modalities differ significantly depending on the site we are assessing and if so, at which sites do we see significant discrepancies? The percent difference was assessed for each measurement taken by the two modalities and the percent difference was averaged by site to depict potential trends in measurement differences by site.

Median BT values reported by physical measurement and micro-CT were plotted for visual comparison and to depict the degree of inter-specimen variation using 95% confidence intervals.

The data for physical measurements taken on the left and right sides of the palate were pooled and represented in a 3D graph for clearer analysis of trends. Studies have indicated no difference between the bone thickness of the right and left sides of the palate therefore pooling of data is acceptable (Gracco, Lombardo, Cozzani, & Siciliani, 2008; Kang et al., 2007; Ryu et al., 2012).

3 Results

3.1 Validation Study Findings

Percent errors from the validation study ranged from 0.34 to 6.69%, with only four of thirty values falling at or above 5%. Average percent errors by site are indicated in Table 1. The average percent error associated with the pin measurement technique fell under 5% and thus satisfied our criteria for accuracy. The intraclass correlation coefficient (ICC = 0.999, $p < 0.01$) indicated excellent repeatability of measurement using the dissection pin and hole measurement technique. The results of the validation study therefore met our predetermined criteria and justified proceeding with this measurement protocol to assess gross anatomical BT measurements.

Table 1- Average Percent Error Associated with Measurements Using Dissection Pin

Site	Percent error (%)
1	1.71
2	1.28
3	1.45
4	2.04
5	4.98
6	2.40

3.2 Descriptive statistics

Descriptive statistics including mean, median, mode, which represent the differences between Micro-CT and Physical measurements for each site are depicted in Table 2.

Table 2 - Descriptive Statistics for Measurement Differences by Site

Site	N	Min	Max	Median	Mean	Std. Error	Std. Deviation
L2	7	-1.40	1.38	0.03	0.24	0.15	1.11
L3	10	-1.38	0.14	-0.90	-0.70	0.15	0.59
L4	9	-0.35	0.38	0.11	0.06	0.86	0.26
PS1	5	-1.38	0.14	0.90	-0.70	0.26	0.26
PS2	10	-.52	3.05	0.25	0.67	0.41	1.29
PS3	10	-0.73	1.00	0.20	0.88	0.16	0.49
PS4	10	-0.29	2.33	0.22	0.44	0.26	0.81
PS5	10	-1.36	0.20	-0.19	-0.24	0.14	0.45
S1	6	-0.29	4.41	0.33	0.97	0.74	1.81
S2	9	-0/35	3.77	0.05	0.43	0.38	1.21
S3	10	-0.16	0.31	0.004	0.044	0.046	0.15
S4	6	-0.25	0.30	0.09	0.03	0.08	0.23
S5	10	-0.34	0.11	-0.01	-0.3	0.04	0.13

3.3 Reliability Between Physical Measurements

Intraclass Correlations revealed excellent reliability (consistency) between physical measurements reported by rater one (ICC =0.993, $p < 0.01$). Figure 19 illustrates this strong, positive, linear relationship between trial one and trial two measurements for rater one. Intraclass Correlations also revealed excellent reliability between the average

measurements reported by rater one and measurements reported by rater two (ICC = 0.983, p<0.01). Figure 20 illustrates the strong, positive, linear relationship between measurements obtained from the two raters. Strong intraclass correlations indicate raters

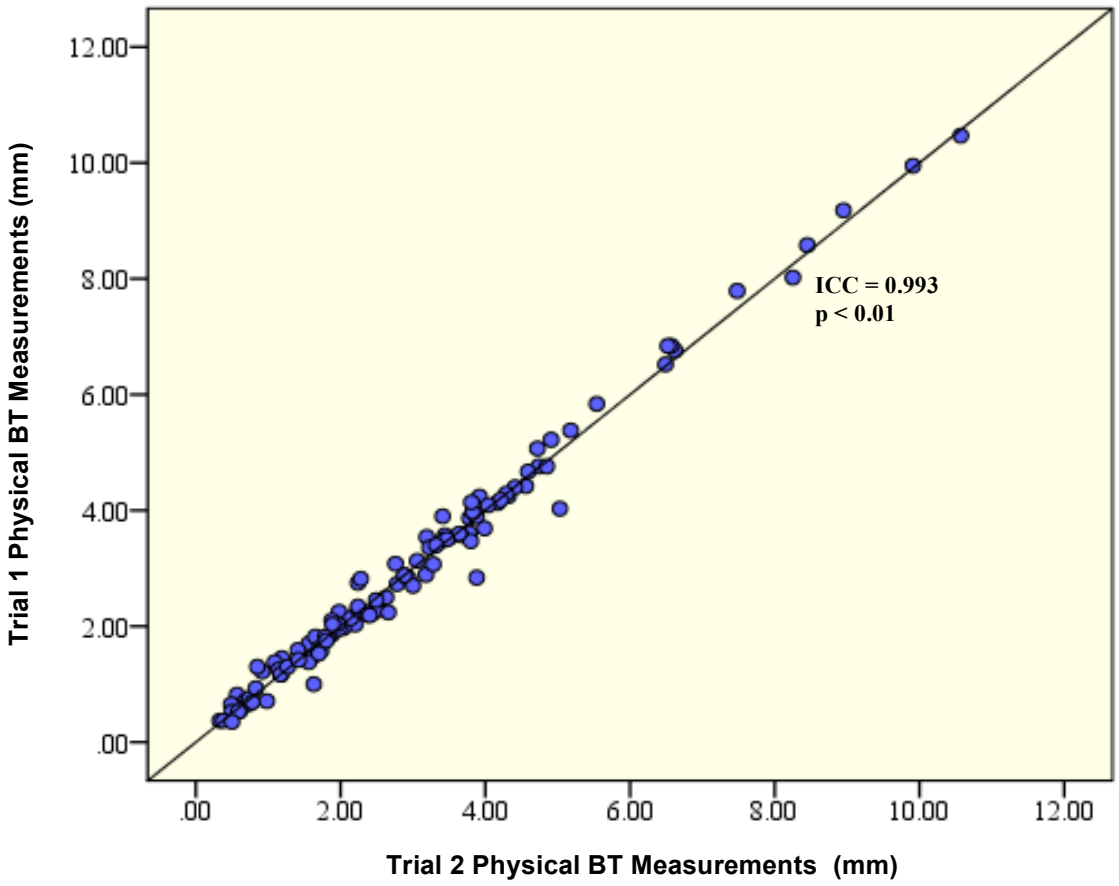

Figure 19 – Intra-rater Reliability for Rater One BT Measurements

had stringently followed protocol (e.g. measured what they had intended to) and that the two raters did so with comparable error since their measurements coincided well with one another in terms of absolute agreement.

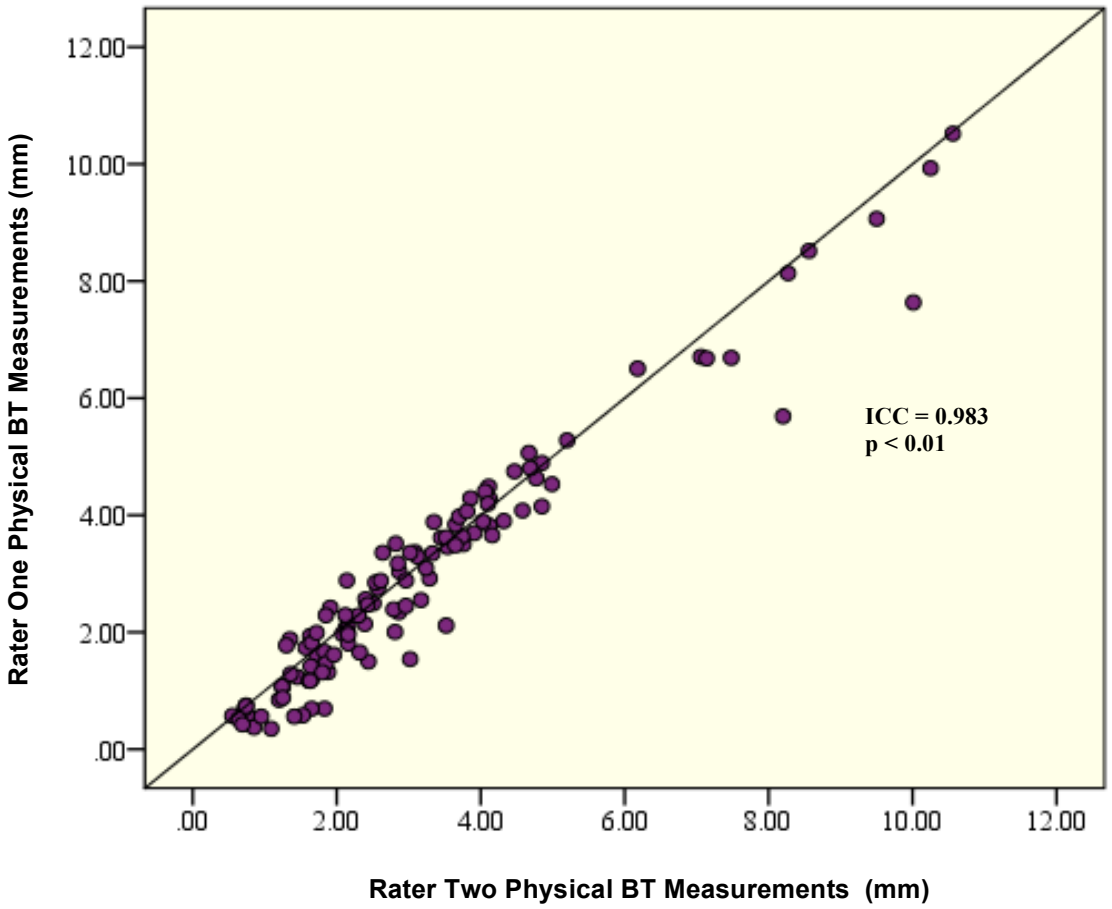

Figure 20 – Inter-rater Reliability for Rater one and Two BT Measurements

3.4 Correlations

Spearman's Rank Correlations, revealed a statistically significant, strong, positive relationship between the two measurement modalities and this held true for comparison between both raters' physical measurements and micro-CT measurements (rater 1: $r_s = 0.948$, $p < 0.01$; rater 2: $r_s = 0.906$, $p < 0.01$). Figures 21 and 22 illustrate the relationship between micro-CT and physical measurements obtained by rater one and rater two, respectively. For those accustomed to linear regressions, Pearson's correlations revealed strong, positive, linear relationships between micro-CT measurements and physical measurements from rater one and two ($r = 0.924$, $p<0.01$; $r=0.879$, $P<0.01$). Due to violation of the assumption of normality typically required for this test, these

correlations may be affected by the positive skew in the data and are likely a conservative estimate of the relationship.

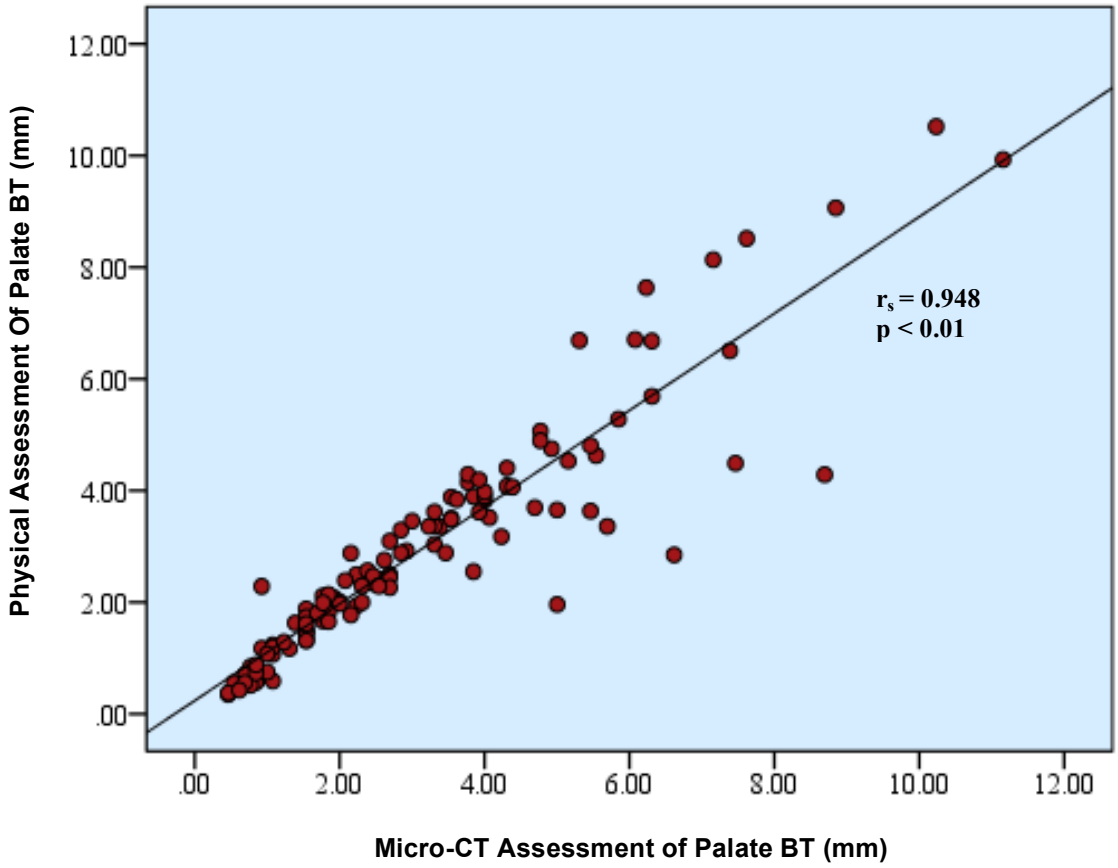

Figure 21 – Relationship between Micro-CT and Rater 1 Physical Measurements of Palate BT

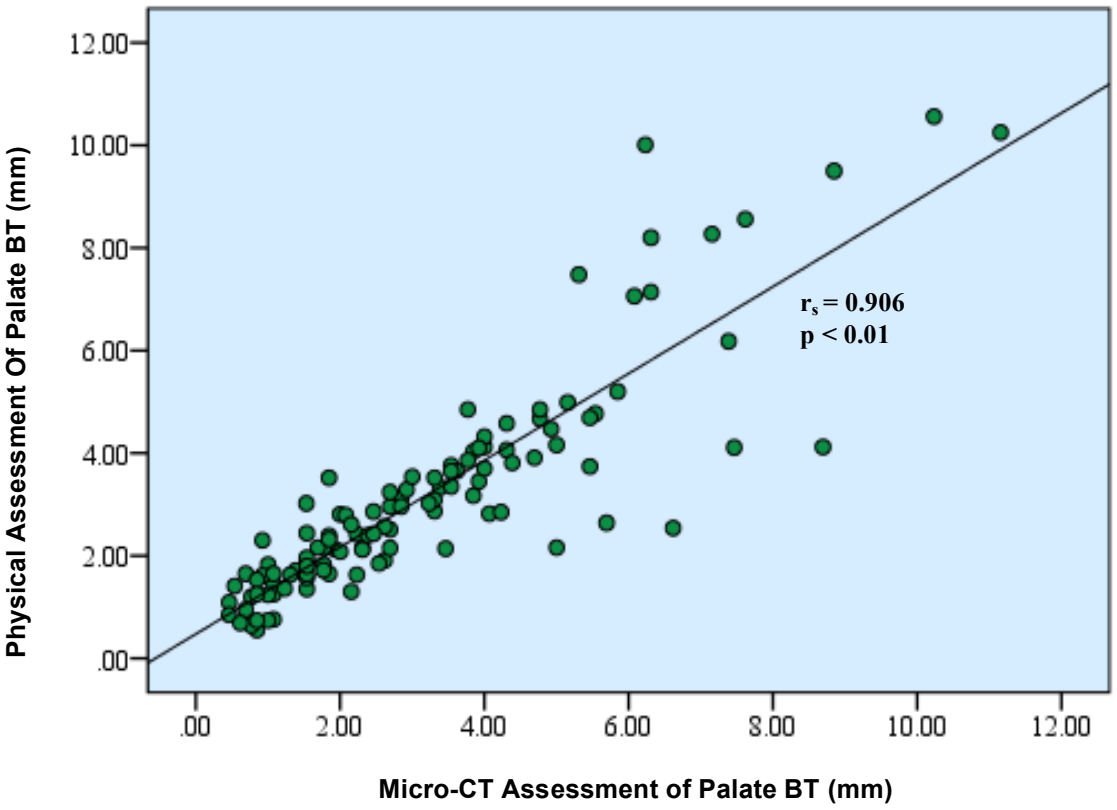

Figure 22 – Relationship between Micro-CT and Rater 2 Physical Measurements of Palate BT

Given that physical measurements obtained by rater one and two were in high agreement with one another and displayed a very similar relationship with respect to micro-CT measurements, the physical data sets were assumed to be equivalent and for efficiency, subsequent statistical analyses were carried out using the averaged data from trial one and two, taken by rater one.

3.5 Measurement Agreement

The standard form of the Bland-Altman plot (Figure 23) reveals valuable information about the difference between micro-CT and physical measurements (rater 1). As expected, majority (95.7%) of differences between measurements compared to their means fell within the limits of agreement defined as 1.96 standard deviations of the mean difference (i.e. ± 1.64 mm), however five points fell above the upper limit of agreement

(+1.96 SD). Upon further examination, it was noted that these points coincide with outliers detected from the box and whisker plots created during tests of normality. These points correspond to measurement differences 3mm or higher, in which micro-CT measurements were greater than anatomical measurements. Given that there were no obvious artifacts in the micro-CT scans, the sites at which these outlying measurement differences arose were visually inspected in the lab to determine whether the morphology of the bone or the wax sealing procedure may have impacted physical measurements. These sites and their description from visual inspection are found in Table 3. Sites at which differences in measurements could be attributed to problems with the physical protocol (such as material in the holes or obvious surface variability around the hole) were excluded from subsequent analysis.

It was noted that for thinner regions of the palate (up to approximately 5 mm), the differences between measurements from the two modalities were clustered close to zero and the mean difference (red reference line, Figure 23) was small (0.18 mm). As measurement values increased, there was a general trend of increasing variation in measurement differences, indicated by larger scatter from the zero line, but almost all values fell at or within two standard deviations of the mean difference which equates to a deviation of $\pm$ 1.64 mm. These appear to be small measurement deviations, until one takes into consideration the very thin bone in the posterior palate ($\leq$ 0.5 mm) and considers what fraction of the screw length (almost one third!) these limits of agreement equate to. The 'limits of agreement' were therefore modified to provide greater insight in terms of agreement between micro-CT and physical measurements with respect to our predetermined definition of agreement (Figure 24).

With the new limits defined as ± 10% of the mean BT, moderate agreement between the two tools is observed, indicated by a large proportion of the measurement differences (approximately half) falling at or within the new limits of agreement. Approximately half of the differences fell outside of the predefined limits however, indicating some level of disparity between the two tools. Disparity between measurements (i.e. differences falling outside of the limits of agreement) was observed for measurements taken at both thick and thin regions of the palate, indicating no systematic trend in measurements disparity.

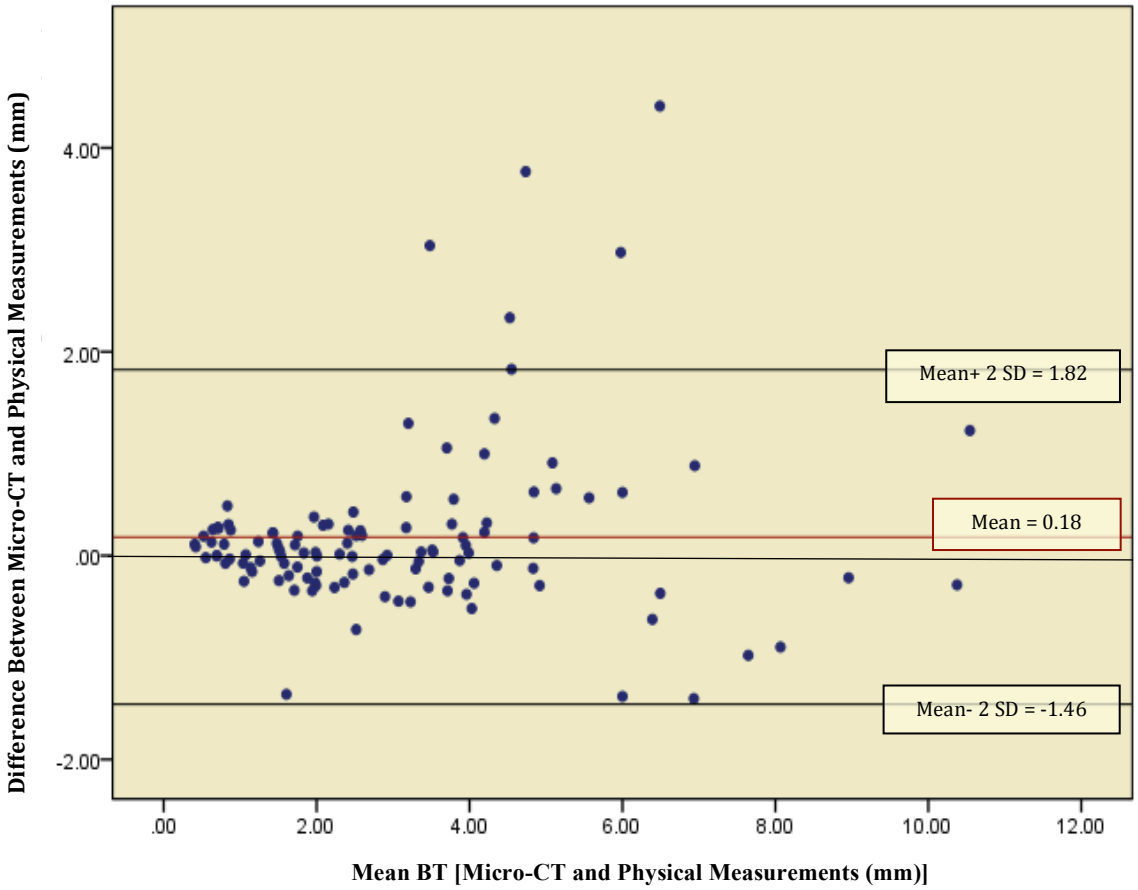

Figure 23 – Agreement between Micro-CT and Gross Anatomical Measurements, Assessed with Traditional Bland-Altman Plot

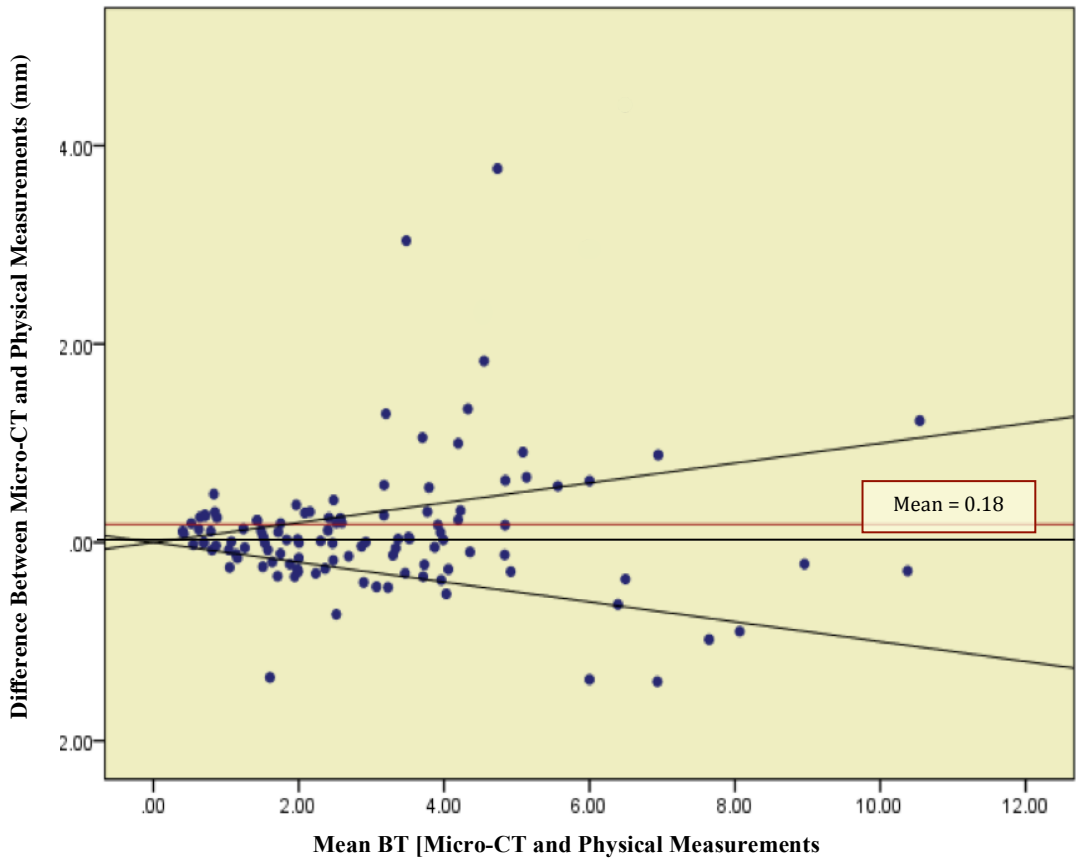

Figure 24 – Agreement between Micro-CT and Gross Anatomical Measurements, Assessed with Modified Limits of Agreement

Table 3 - Outlying Measurements and Visual Inspection of Site

Specimen	Site	Measurement Difference (mm)	Visual Inspection of Site
1517	PS2	2.97 (μCT > Physical)	Small dip in bone anterior to hole, bony surface around hole is irregular (bumpy)
	S1	4.41 (μCT > Physical)	Slight lifting of tape at anterior surface of nasal cavity (close to site) may cause wax penetration into hole; severe curvature of palate at this location (BT anterior to hole > posterior)
1605	PS4	2.33 (μCT > Physical)	Dark speck observed at nasal end of hole (potential foreign material in hole)
1683	PS2	3.04 (μCT > Physical)	No visible materials in hole; no obvious irregularity of bone surface near hole
1719	S2	3.77 (μCT > Physical)	Hole extended with larger screw; unable to observe if wax penetrated (deep hole)

The Kruskall Wallis H test ($\alpha = 0.05$) indicated that no statistically significant differences existed across the sites in terms of measurement differences ($p > 0.05$). SPSS output from the Kruskall Wallis test can be found in Appendix H. This finding, however, was unexpected given the observed range in the average percent differences between the measurements (6.45- 28.8 %), seen in Table 4.

As seen in Table 4, high percent differences between micro-CT and physical measurements were observed. The largest percent differences (approximately 20% or greater) resulted at sites: S1, PS2, S2, L3 and L4. These sites were generally the most anterior or lateral sites assessed, (with the exception of PS1) and were located in areas of curvature; those being the anterior curvature of the palate or the lateral curvature as the palate transitions to alveolar bone.

Table 4 - Percent Differences between Micro-CT and Anatomical Measurements by Site

Measurement Site	Average Percent Difference (%)	Sample size
PS1	12.1	n = 5
S1	24.2	n = 6
PS2	28.8	n = 10
S2	22.2	n = 10
L2	20.7	n = 7
PS3	12.1	n = 10
S3	10.8	n = 10
L3	19.9	n = 10
PS4	17.2	n = 10
S4	18.9	n = 9
L4	24.1	n = 9
PS5	13.2	n =10
S5	6.45	n = 10

Graphically, when comparing median bone thickness measurements taken by the two modalities for each site, (Figure 25) similarity between measurements is very clear. It should be cautioned, however, that just because the measurements are not statistically significant, this does not mean that clinically significant differences are absent since statistical tests do not comprehend the specific problem we are trying to solve (Bland & Altman, 1999). When comparing micro-CT and gross anatomical measurement of palate BT, large inter-specimen variability is noted for the most anterior and also very curved sites (S1, PS1, L2) as indicated by the large confidence intervals.

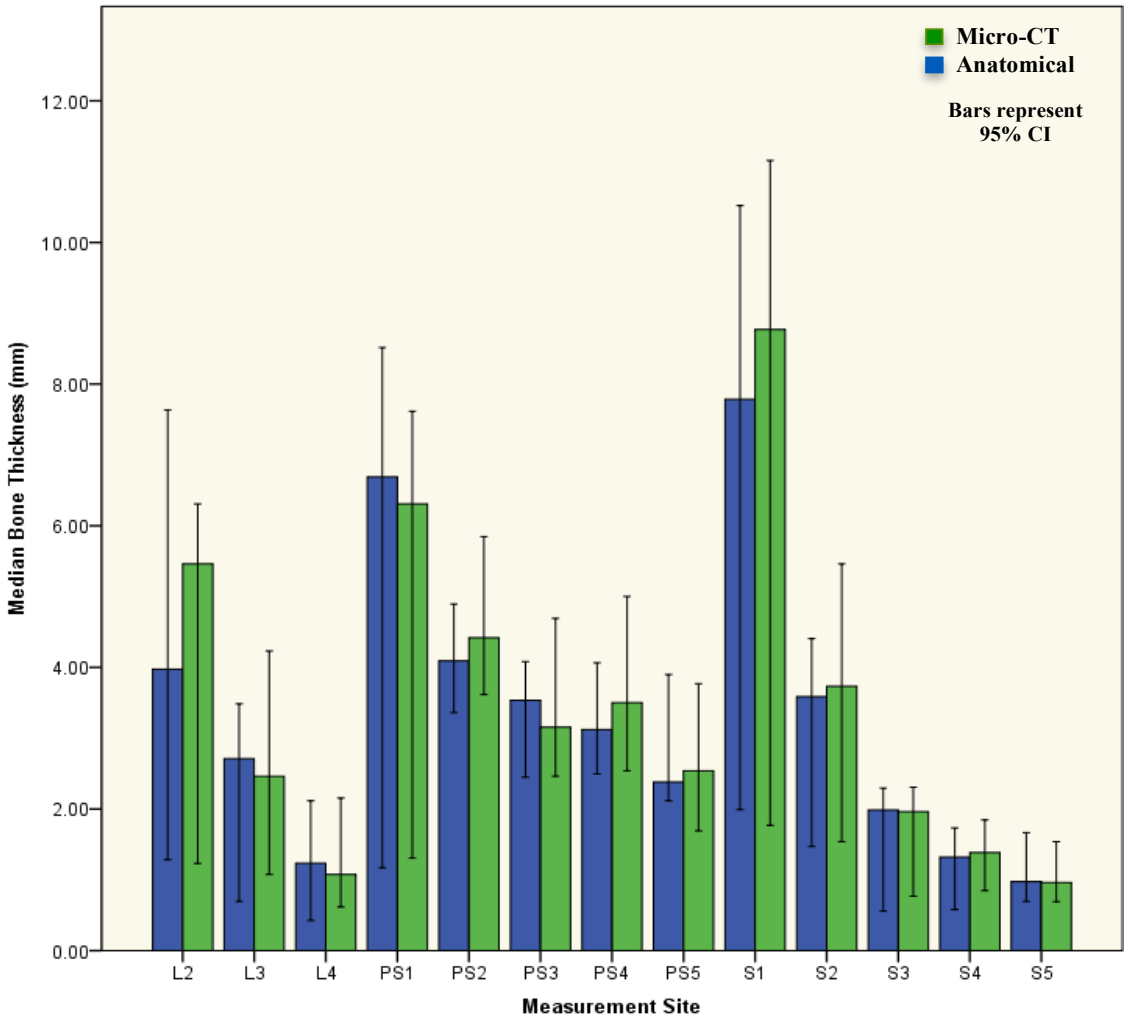

Figure 25 - Comparison of Median BT Values Reported by Micro-CT and Physical Measurements

As seen in Figure 26, 3D graphical representation of mean BT by site, obtained from anatomical measurements, indicates a general trend of thinning from anterior to posterior, with parasagittal sites (indicated by the green and purple bars) remaining thicker at more posterior regions of the palate than sagittal sites and lateral sites. Palate BT was also noted to show an 'hourglass' trend when comparing parasagittal, sagittal and lateral sites located the same distance from the incisive foramen according to the grid used; parasagittal sites were thicker than corresponding sagittal sites and lateral sites were thicker than corresponding sagittal sites. In other words, thinning was observed from parasagittal to sagittal and thickening from sagittal to lateral.

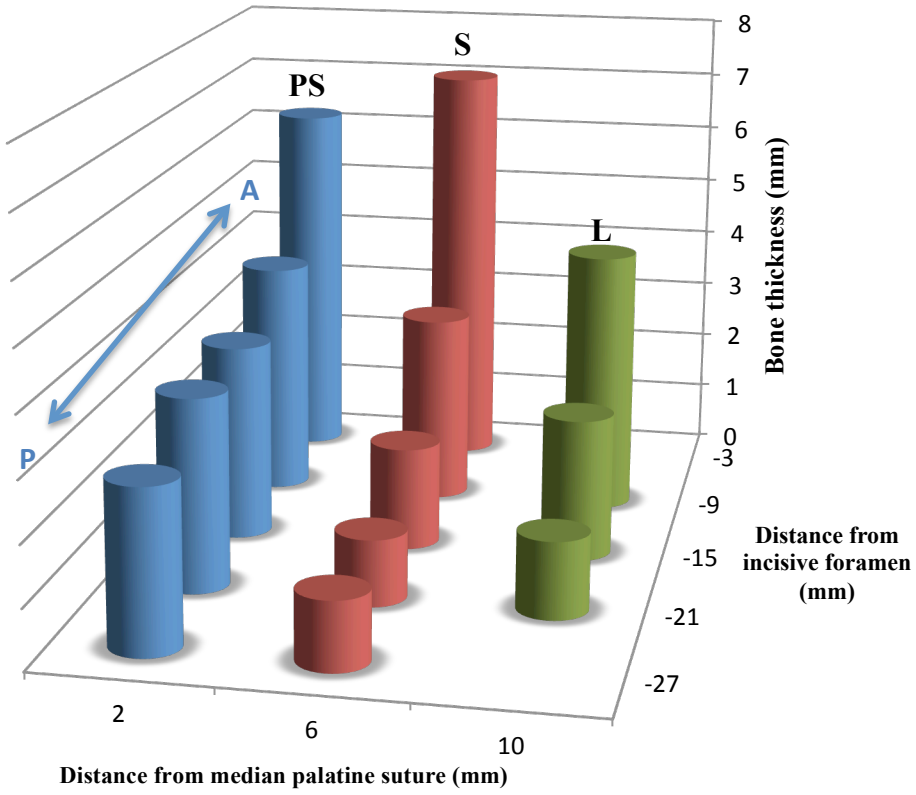

Figure 26 – Mean Anatomical Bone Thickness by Site

L, **S**, and **PS** represent lateral, sagittal, and parasagittal sites on the hard palate; A and P labels indicate anterior and posterior orientation in terms of palate anatomy

4 Discussion

As the use of orthodontic miniscrews has increased in the hard palate, bone thickness of the palate, namely in the anterior and paramedian regions has been extensively studied with in-vivo imaging techniques, such as lateral cephalogram and CBCT (Baumgaertel, 2011; Farnsworth et al., 2011; Gracco et al., 2008, 2007; Jung, Wehrbein, Heuser, & Kunkel, 2011b; Ryu et al., 2012; Wehrbein et al., 1999). Limited cadaveric (in-vitro) research exists on this topic, however, and there is a marked lack of gross anatomical studies, (Winsauer et al., 2014) which could validate the accuracy of measurements obtained by imaging methods.

Of the few non-imaging cadaveric studies, histology has been the choice of assessment (Stockmann et al., 2009; Wehrbein, 2008, 2009). Micro-CT, however, has been found to be comparable to histological investigation with respect to the study of trabecular bone structure (Kuhn et al., 1990) and is a much more efficient means of assessment (Guldberg et al., 2003). Prior to investigation by Bourassa (2015) high resolution micro-CT imaging has not been used to quantify the hard palate, yet its use as an accurate research tool has been documented for applications such as evaluation of enamel thickness of teeth (Swain & Xue, 2009), measurements of the posterior edentulous maxilla for the placement of dental implants (Israel, 2011) and measurements of bony trabeculae (Buchman et al., 1998; Kuhn et al., 1990). The purpose of this study was therefore to compare measurements of bone thickness obtained using high-resolution micro-CT to gross anatomical measurements of the cadaveric bone to determine whether micro-CT provides a comparable quantification of hard palate thickness to the true anatomy and can therefore be used as a research tool with the application of orthodontic miniscrews in mind.

Cadaveric research possesses intrinsic limitations relating to the age and rarity of human donors. Concern arose that the age of the donors (mean age 77.6 years) used in this study may have influenced the quantity/ thickness of bone reported. However after, assessing the literature comparing bone thickness of the palate across various ages, it does not

appear that age has a significant effect except in the youngest individuals assessed. Ryu and colleagues (2012) have indicated statistically significant differences in the bone thickness of children with early mixed dentition (i.e. deciduous and some permanent teeth) compared to children with late mixed dentition and young adults with permanent dentition. Children with early mixed dentition (mean age 8.03 ± 0.93 years) were reported to have significantly lower hard palate bone thickness, especially in the anterior regions of the palate compared to the latter groups. Gracco and colleagues (2008) however, found no statistically significant differences when comparing subjects of a wider range of ages (10-15, 15-20 and 20-44 years) with the exception of one site (16 mm posterior to the incisive foramen and 6 mm adjacent to the median palatine suture). Bone thickness in both of these studies was found to decrease from anterior to posterior with the thickest bone in the anterior region at the median palatine suture and paramedian regions adjacent to the suture. The same trends was observed in a study assessing the bone thickness of the hard palate in adults 18-35 years (Kang et al., 2007). In light of these findings it appears that the morphology of the palate does not differ significantly with age once subjects reach the stage of late mixed dentition.

Where age likely plays a role is its association with partial loss of teeth or edentulism given that the average number of maxillary teeth in this study was 9.9. Although Cawood & Howell (1988) have indicated that unlike the alveolar process, the palate does not change shape (thickness) significantly with edentulism, visual inspection of an edentulous maxillae in the Western University gross anatomy lab indicated very paper-thin regions of the palate closest to the alveolar process and an overall thinner appearance of the hard palate. Therefore, it is predicted that partial edentulism may have impacted bone thickness measurements. However, this factor does not impact the study's primary focus to compare two measurement modalities and assess micro-CT suitability for measuring the hard palate. In the case of reporting general thickness trends in the palate, this factor may result in some measurements being thinner than what may have been observed had subjects possessed their full dentition, nonetheless, the values reported represent the minimum available bone (rather than an overestimation) and are therefore still of value when considering OMS placement.

The rarity of human donors is another limitation, in that the sample size used in the study (n = 10) was relatively small. Should a larger sample size have been obtained there is the potential that statistically significant differences in measurements between sites may have been detected.

Regarding measurement disparity, the largest percentage errors reported appear to be associated with palate curvature either anteriorly or laterally. Extension of the OMS holes by a longer and wider miniscrew was theorized to potentially impact error between measurements, because it may allow the dissection pin to be angled slightly differently than sites at which no extension took place. However, of the five sites with the highest percentage error between measurement modalities, site S1 was the only site extended (for four specimens), therefore the high percentage errors noted for these five sites were not primarily due to hole extension. The high percentage errors that resulted were most likely due to the influence of curvature on the physical measurements.

Dissection pins were consistently marked at the anterior side of the hole and due to the curvature or sloping of the palate, physical measurements may have resulted in an overestimation of thickness, given that micro-CT measurements were taken directly at the mid-point of the hole. A closer approximation of physical palatal thickness in the anterior palate may have resulted if measurements were made with the pin marked at both the anterior of the hole and again at the posterior of the hole and the two values averaged to better represent a measurement at the midpoint of the hole, however, time limitations did not permit for a replication of measurements.

Regardless whether pins are marked at the anterior or posterior of the hole, however, marking the pin at the *periphery* of the hole for a measurement of the thickness *directly at the hole* may introduce measurement error if the bone surface surrounding the hole is very irregular. Measurements obtained by marking the pin at the periphery of an OMS hole could be impacted by a dip or ridge in the bone immediately anterior to the hole, potentially leading to under- or overestimates of anatomical bone thickness compared to micro-CT measures at the same site.

An additional limitation lies in the design of the pilot study. The method used to evaluate the proposed physical measurement technique was an 'ideal case' scenario in which the surface of the measured item (cedar wedge) was smooth (unlike the pitted, bumpy surface of the palate) and its curvature was not as extreme as that observed in the anterior palate of most some specimens. The hockey tape used to block the OMS holes also remained more securely fastened to the wood whereas in the bone, lifting of the tape may have led to the seepage of wax into some measurements sites. Therefore it is cautioned that this validation was likely not a close enough approximation to the true anatomy in order to satisfactorily validate the physical measurement technique. Percent errors remained low in the validation study; however, the uneven surface anatomy of the palate may have complicated physical measurements, leading to increased measurement error, thereby ruling out the pin measurement technique as a "gold standard" for measurement comparison. Furthermore, the high inter-and intra-rater reliability observed for physical measurements indicates that the raters did not negatively influence the measurements because they followed protocol. Again, this reinforces our concerns that potential limitations existed within the physical measurement protocol itself.

Despite the limitations of the study, results indicated a strong positive relationship between micro-CT and anatomical measurements of palate thickness, as well as a moderate degree of agreement between micro-CT and gross anatomical measurements. Bland and Altman (1999) stress that some amount of disagreement between measurements is unavoidable, as even 'gold standard' measurements are not completely error free, thus, perfect agreement would never be expected. Due to limitations with the anatomical protocol and micro-CT modalities with much higher resolution do exist, the findings of the study neither dismiss nor advocate the general use of micro-CT for measurements of the palate.

Previous studies have indicated Micro-CT produces measurements that are highly comparable to histological examination of bone (Buchman et al., 1998, Gielkens et al., 2008; Kuhn, Goldstein, Feldkamp, Goulet, & Jesion, 1990), however, these studies relied on micro-CT scanners with a higher resolution than that used in this study (E.g. resolutions of 40 microns for cranial specimens, 50-70 microns for various bony

specimens and an isotropic voxel size of 48 microns, respectively). The scanning resolution used in the present study 180 microns (0.18 mm) was markedly larger than that used in histological comparison studies as was the isotropic voxel size of 150 microns (0.15 mm). Comparability to histological measurements lead us to hypothesize that a high level of agreement would be seen with respect to gross anatomical measurements, however, the resolution of the scanner used in the present study may have limited our comparison. Using a scanner with smaller voxel sizing and increased resolution may provide a more representative 3D image of the hard palate when compared to the physical anatomy.

A number of differences between micro-CT and physical measurements fell outside the defined limits of agreement but this was observed for *both* thick and thin regions of the palate. Potential errors were expected for micro-CT measurements at *thinner* regions of the palate since very thin bone is closer to the limits of resolution of micro-CT and this trend was not observed. If a tool was systematically inaccurate we would expect to see more consistent differences between the two measurements (e.g. micro-CT would either consistently over or underestimate thickness compared to physical measurements), however, there was no general trend indicating this. Therefore, it is predicted that the differences observed between measurements may be at least in part due to inaccuracies in physical measurements and the resolution of the micro-CT scanner thus, we cannot draw a definitive conclusion about the suitability of micro-CT for imaging the hard palate.

Future studies should utilize a higher resolution micro-CT scanner and develop a more stringent technique for gross anatomical assessment of the hard palate, in order to minimize measurement errors and allow for a more objective comparison between measurements. Clinically, micro-CT would never be used on live patients, however, if micro-CT provides an accurate representation of hard palate thickness, it would be of great insight to compare it to clinically applicable cone beam computed tomography in order to objectively assess whether this clinical tool yields precise measurements and is therefore applicable for preclinical assessment prior to miniscrew insertion.

Gross anatomical measurements of the hard palate indicated that bone thickness or quality varied by site. The general trends observed are a thinning from anterior to posterior, and lateral thinning when comparing parasagittal to sagittal sites. These finding are in agreement with current literature (Baumgaertel, 2009; Farnsworth et al., 2011; Gracco et al., 2008; Kang et al., 2007; Ryu et al., 2012). Subsequent thickening from sagittal to lateral regions was also observed and is consistent with the findings of Baumgaertel (2009). Similar to the findings of Ryu and colleagues (2012), parasagittal sites tended to be the thickest overall with the exception of the most anterior site (closest to the incisive foramen).

5 Conclusions

Despite the differences observed between the two modalities at some sites and a large range in measurements differences, we cannot conclude whether or not micro-CT is a comparable means for hard palate assessment, on the grounds that anatomical measurements may not have been the 'gold standard' for comparison in this case. According to the general trends of bone thickness observed for the hard palate, parasagittal and sagittal sites 3 mm posterior to the incisive foramen on average provide sufficient to fully engage a 6mm miniscrew. OMS placement at these anterior sites would be appropriate based on available bone thickness. If minor nasal perforation is not of large concern to the clinician, OMSs could also be placed along the parasagittal region of the palate.

6 References

Adams, J. E. (2009). Quantitative computed tomography. *European Journal of Radiology*, *71*(3), 415–424. doi:10.1016/j.ejrad.2009.04.074

Bagi, C. M., Hanson, N., Andresen, C., Pero, R., Lariviere, R., Turner, C. H., & Laib, A. (2006). The use of micro-CT to evaluate cortical bone geometry and strength in nude rats: Correlation with mechanical testing, pQCT and DXA. *Bone*, *38*(1), 136–144. doi:10.1016/j.bone.2005.07.028

Baumgaertel, S. (2009). Quantitative investigation of palatal bone depth and cortical bone thickness for mini-implant placement in adults. *American Journal of Orthodontics and Dentofacial Orthopedics : Official Publication of the American Association of Orthodontists, Its Constituent Societies, and the American Board of Orthodontics*, *136*(1), 104–8. doi:10.1016/j.ajodo.2008.11.020

Baumgaertel, S. (2011). Cortical bone thickness and bone depth of the posterior palatal alveolar process for mini-implant insertion in adults. *American Journal of Orthodontics and Dentofacial Orthopedics : Official Publication of the American Association of Orthodontists, Its Constituent Societies, and the American Board of Orthodontics*, *140*(6), 806–11. doi:10.1016/j.ajodo.2011.05.020

Berkovitz, B. K. B., Moxham, B. J., & Holland, G. R. (2009). *Oral anatomy, histology and embryology*. (A. Taylor & L. Stader, Eds.) (4th ed.). Mosby Elsevier. Retrieved from http://scholar.google.com/scholar?hl=en&btnG=Search&q=intitle:Oral+Anatomy+Histology+and+Embryology#0

Bland, J. M., & Altman, D. G. (1986). Statistical methods for assessing agreement between two methods of clinical measurement. *Lancet*, *1*(8476), 307–310. doi:10.1016/S0140-6736(86)90837-8

Bland, J. M., & Altman, D. G. (1999). Measuring agreement in method comparison studies. *Statistical Methods in Medical Research*, *8*(2), 135–160. doi:10.1191/096228099673819272

Bourassa, C. (2015). An In-Vitro Comparison of Different Palatal Sites for Orthodontic Miniscrew Insertion : The Effect of Bone Quality and Quantity on Primary Stability. *University of Western Ontario - Electronic Thesis and Dissertation Repository. Paper 2672.*

Buchman, S. R., Sherick, D. G., Goulet, R. W., & Goldstein, S. a. (1998). Use of microcomputed tomography scanning as a new technique for the evaluation of membranous bone. *The Journal of Craniofacial Surgery*. doi:10.1097/00001665-199801000-00011

Cawood, J. I., & Howell, R. a. (1988). A classification of the edentulous jaws. *International Journal of Oral and Maxillofacial Surgery*, *17*(4), 232–236. doi:10.1016/S0901-5027(88)80047-X

Chang, Y.J., Lee, H.S., Chun, Y. S. (2004). Microscrew Anchorage ffor Molar Intrusion. *Journal of Clinical Orthodontics*, *38*, 325–330.

Cheng, S.-J., Tseng, I.-Y., Lee, J.-J., & Kok, S.-H. (2004). A prospective study of the risk factors associated with failure of mini-implants used for orthodontic anchorage. *The International Journal of Oral & Maxillofacial Implants*, *19*(1), 100–106.

Crismani, A. G., Bertl, M. H., Celar, A. G., Bantleon, H.-P., & Burstone, C. J. (2010). Miniscrews in orthodontic treatment: review and analysis of published clinical trials. *American Journal of Orthodontics and Dentofacial Orthopedics : Official Publication of the American Association of Orthodontists, Its Constituent Societies, and the American Board of Orthodontics*, *137*(1), 108–113. doi:10.1016/j.ajodo.2008.01.027

Day, T. A., & Girod, D. A. (Eds.). (2006). *Oral Cavity Reconstruction*. New York: Taylor and Francis Group.

Deguchi, T., Nasu, M., Murakami, K., Yabuuchi, T., Kamioka, H., & Takano-Yamamoto, T. (2006). Quantitative evaluation of cortical bone thickness with computed tomographic scanning for orthodontic implants. *American Journal of Orthodontics and Dentofacial Orthopedics : Official Publication of the American Association of Orthodontists, Its Constituent Societies, and the American Board of Orthodontics*, *129*(6), 721.e7–12. doi:10.1016/j.ajodo.2006.02.026

Drake, R., Vogl, A., & Mitchell, A. (2015). *Gray's Anatomy For Students* (3rd ed.). Philadelphia.

Du, L. Y., Umoh, J., Nikolov, H. N., Pollmann, S. I., Lee, T.-Y., & Holdsworth, D. W. (2007). A quality assurance phantom for the performance evaluation of volumetric micro-CT systems. *Physics in Medicine and Biology*, *52*(23), 7087–7108. doi:10.1088/0031-9155/52/23/021

Edgell, S. E., & Noon, S. M. (1984). Effect of violation of normality on the t test of the correlation coefficient. *Psychological Bulletin*, *95*, 576–583. doi:10.1037/0033-2909.95.3.576

Farnsworth, D., Rossouw, P. E., Ceen, R. F., & Buschang, P. H. (2011). Cortical bone thickness at common miniscrew implant placement sites. *American Journal of Orthodontics and Dentofacial Orthopedics : Official Publication of the American Association of Orthodontists, Its Constituent Societies, and the American Board of Orthodontics*, *139*(4), 495–503. doi:10.1016/j.ajodo.2009.03.057

Feldkamp, L. a, Goldstein, S. a, Parfitt, a M., Jesion, G., & Kleerekoper, M. (1989). The direct examination of three-dimensional bone architecture in vitro by computed tomography. *Journal of Bone and Mineral Research : The Official Journal of the American Society for Bone and Mineral Research*, *4*(1), 3–11. doi:10.1002/jbmr.5650040103

Galil, K. (2004). Retrieved July 5, 2014, from http://www.forestcity.ca/drgalil/skull/index.htm

Gielkens, P. F. M., Schortinghuis, J., de Jong, J. R., Huysmans, M. C. D. N. J. M., Leeuwen, M. B. M. Van, Raghoebar, G. M., … Stegenga, B. (2008). A comparison of micro-CT, microradiography and histomorphometry in bone research. *Archives of Oral Biology*, *53*(6), 558–566. doi:10.1016/j.archoralbio.2007.11.011

Gracco, A., Lombardo, L., Cozzani, M., & Siciliani, G. (2008). Quantitative cone-beam computed tomography evaluation of palatal bone thickness for orthodontic miniscrew placement. *American Journal of Orthodontics and Dentofacial Orthopedics : Official Publication of the American Association of Orthodontists, Its Constituent Societies, and the American Board of Orthodontics*, *134*(3), 361–9. doi:10.1016/j.ajodo.2007.01.027

Gracco, A., Luca, L., Cozzani, M., & Siciliani, G. (2007). Assessment of palatal bone thickness in adults with cone beam computerised tomography. *Australian Orthodontic Journal*, *23*(2), 109–13. Retrieved from http://www.lucalombardo.net/download/articoli/7(2).pdf

Guldberg, R. E., Ballock, R. T., Boyan, B. D., Duvall, C. L., Lin, A. S., Nagaraja, S., … Taylor, W. R. (2003). Analyzing bone, blood vessels, and biomaterials with microcomputed tomography. *IEEE Engineering in Medicine and Biology Magazine*, *22*(5), 77–83. doi:10.1109/MEMB.2003.1256276

Hassanali, J., & Mwaniki, D. (1984). Palatal analysis and osteology of the hard palate of the Kenyan African skulls. *The Anatomical Record*, *209*(2), 273–280. doi:10.1002/ar.1092090213

Henriksen, B., Bavitz, B., Kelly, B., & Harn, S. D. (2003). Evaluation of bone thickness in the anterior hard palate relative to midsagittal orthodontic implants. *The International Journal of Oral & Maxillofacial Implants*, *18*(4), 578–581.

Holdsworth, D. W., & Thornton, M. M. (2002). Micro-CT in small animal and specimen imaging. *Trends in Biotechnology*, *20*(8), S34–S39. doi:10.1016/S0167-7799(02)02004-8

Huang, L.-H., Shotwell, J. L., & Wang, H.-L. (2005). Dental implants for orthodontic anchorage. *American Journal of Orthodontics and Dentofacial Orthopedics : Official Publication of the American Association of Orthodontists, Its Constituent Societies, and the American Board of Orthodontics*, *127*(6), 713–22. doi:10.1016/j.ajodo.2004.02.019

IBM. (2012). The Bland-Altman Plot. Retrieved April 1, 2015, from https://www-304.ibm.com/support/docview.wss?uid=swg21476730

Israel, E. (2011). *An anatomical study of the alveolar process in the human maxilla and its relation to the maxillary sinus using μ- CT: implications toward dental implant success*. Western University.

Ito, M. (2005). Assessment of bone quality using micro-computed tomography (micro-CT) and synchrotron micro-CT. *Journal of Bone and Mineral Metabolism*, *23*(S1), 115–121. doi:10.1007/BF03026335

Jiang, Y., Zhao, J., Liao, E. Y., Dai, R. C., Wu, X. P., & Genant, H. K. (2005). Application of micro-ct assessment of 3-d bone microstructure in preclinical and clinical studies. *Journal of Bone and Mineral Metabolism*, *23*(SUPPL. 1), 122–131. doi:10.1007/BF03026336

Jung, B. a., Wehrbein, H., Heuser, L., & Kunkel, M. (2011a). Vertical palatal bone dimensions on lateral cephalometry and cone-beam computed tomography: Implications for palatal implant placement. *Clinical Oral Implants Research*, *22*, 664–668. doi:10.1111/j.1600-0501.2010.02021.x

Jung, B. a., Wehrbein, H., Heuser, L., & Kunkel, M. (2011b). Vertical palatal bone dimensions on lateral cephalometry and cone-beam computed tomography: Implications for palatal implant placement. *Clinical Oral Implants Research*, *22*(6), 664–668. doi:10.1111/j.1600-0501.2010.02021.x

Kalender, W. A., Deak, P., & Engelke, K. (2011). *Small Animal Imaging*. (F. Kiessling & B. J. Pichler, Eds.). Berlin, Heidelberg: Springer Berlin Heidelberg. doi:10.1007/978-3-642-12945-2

Kang, S., Lee, S.-J., Ahn, S.-J., Heo, M.-S., & Kim, T.-W. (2007). Bone thickness of the palate for orthodontic mini-implant anchorage in adults. *American Journal of Orthodontics and Dentofacial Orthopedics : Official Publication of the American Association of Orthodontists, Its Constituent Societies, and the American Board of Orthodontics*, *131*(4 Suppl), S74–81. doi:10.1016/j.ajodo.2005.09.029

Kiessling, F., Pichler, B., & Hauff, P. (Eds.). (2010). *Small Animal Imaging: Basics and Practical Guide*. Springer-Verlag Berlin Heidelberg. doi:101pp7978364212945-2

Kim, H.-J., Yun, H.-S., Park, H.-D., Kim, D.-H., & Park, Y.-C. (2006). Soft-tissue and cortical-bone thickness at orthodontic implant sites. *American Journal of Orthodontics and Dentofacial Orthopedics : Official Publication of the American Association of Orthodontists, Its Constituent Societies, and the American Board of Orthodontics*, *130*(2), 177–82. doi:10.1016/j.ajodo.2004.12.024

Kim, Y. H., Yang, S.-M., Kim, S., Lee, J. Y., Kim, K. E., Gianelly, A. a, & Kyung, S.-H. (2010). Midpalatal miniscrews for orthodontic anchorage: factors affecting clinical success. *American Journal of Orthodontics and Dentofacial Orthopedics : Official Publication of the American Association of Orthodontists, Its Constituent Societies, and the American Board of Orthodontics*, *137*(1), 66–72. doi:10.1016/j.ajodo.2007.11.036

King, K. S., Lam, E. W., Faulkner, M. G., Heo, G., & Major, P. W. (2007). Vertical bone volume in the paramedian palate of adolescents: a computed tomography study. *American Journal*

of Orthodontics and Dentofacial Orthopedics : Official Publication of the American Association of Orthodontists, Its Constituent Societies, and the American Board of Orthodontics, *132*(6), 783–8. doi:10.1016/j.ajodo.2005.11.042

Klosek, S. K., & Rungruang, T. (2009). Anatomical study of the greater palatine artery and related structures of the palatal vault: Considerations for palate as the subepithelial connective tissue graft donor site. *Surgical and Radiologic Anatomy*, *31*(4), 245–250. doi:10.1007/s00276-008-0432-4

Kravitz, N.D., Kusnoto, B., Tsay, T.P., hohlt, W. F. (2007). The Use of Temporary Anchorage Devices for Molar Intrusion. *Journal of the American Dental Association*, *138*(1), 56–64.

Kuhn, J. L., Goldstein, S. a, Feldkamp, L. a, Goulet, R. W., & Jesion, G. (1990). Evaluation of a microcomputed tomography system to study trabecular bone structure. *Journal of Orthopaedic Research : Official Publication of the Orthopaedic Research Society*, *8*(6), 833–842. doi:10.1002/jor.1100080608

Kyung, S. H., Hong, S. G., & Park, Y. C. (2003). Distalization of Maxillary Molars with a Midpalatal Miniscrew. *Journal of Clinical Orthodontics*, *37*, 22–26.

Kyung, S.-H., Lee, J. Y., Shin, J. W., Hong, C., Dietz, V., & Gianelly, A. a. (2009). Distalization of the entire maxillary arch in an adult. *American Journal of Orthodontics and Dentofacial Orthopedics : Official Publication of the American Association of Orthodontists, Its Constituent Societies, and the American Board of Orthodontics*, *135*(4 Suppl), S123–32. doi:10.1016/j.ajodo.2008.01.015

Lombardo, L., Gracco, A., Zampini, F., Stefanoni, F., & Mollica, F. (2010). Optimal Palatal Configuration for Miniscrew Applications, *80*(1). doi:10.2139/122908-662.1

Ludwig, B., Glasl, B., Kinzinger, G. S. M., Lietz, T., & Lisson, J. a. (2011). Anatomical guidelines for miniscrew insertion: Vestibular interradicular sites. *Journal of Clinical Orthodontics : JCO*, *45*(3), 165–173.

Mamourian, A. C. (2013). *CT Imaging: Practical Physics, Artifacts, and Pitfalls*. New York: Oxford University Press, USA. Retrieved from https://books.google.ca/books?id=yFxpAgAAQBAJ

McDonald, J. H. (2014). *Handbook of Biological Statistics* (3rd ed.). Baltimore: Sparky House Publishing. Retrieved from http://www.biostathandbook.com/wilcoxonsignedrank.html

Mizrahi, E., & Mizrahi, B. (2007). Mini-screw implants (temporary anchorage devices): orthodontic and pre-prosthetic applications. *Journal of Orthodontics*, *34*(2), 80–94. doi:10.1179/146531207225021987

Moore, K. ., Agur, A. M., & Dalley, A. F. (2011). *Essential Clinical Anatomy* (4th ed.). Baltimore: Lippincott, Williams, & Wilkins.

Netter, F. H. (2014). *Atlas of Human Anatomy* (Sixth.). Philadelphia: Elsevier Saunders.

Norton, N. S. (2012). *Netter's Head and Neck Anatomy for Dentistry* (2nd ed.). Philadelphia: Elsevier Saunders.

Novelline, R. (1997). *Squire's Fundamentals of Radiology* (5th ed.). Cambridge: Harvard University Press.

Papadopoulos, M. a, & Tarawneh, F. (2007). The use of miniscrew implants for temporary skeletal anchorage in orthodontics: a comprehensive review. *Oral Surgery, Oral Medicine, Oral Pathology, Oral Radiology, and Endodontics*, *103*(5), e6–15. doi:10.1016/j.tripleo.2006.11.022

Papageorgiou, S. N., Zogakis, I. P., & Papadopoulous, M. A. (2012). Failure rates and Associated Risk factors of Orthodontic Miniscres Implant: A Meta Analysis. *American Journal of Orthodontics and Dentofacial Orthopedics*, *142*(5), 577–595e7.

Payne, J. T. (1978). Introduction To CT Physics. *Journal of Computer Assisted Tomography*, *2*(2), 236. doi:10.1097/00004728-197804000-00024

Piagkou, M., Xanthos, T., Anagnostopoulou, S., Demesticha, T., Kotsiomitis, E., Piagkos, G., … Johnson, E. O. (2012). Anatomical variation and morphology in the position of the palatine foramina in adult human skulls from Greece. *Journal of Cranio-Maxillofacial Surgery*, *40*(7), e206–e210. doi:10.1016/j.jcms.2011.10.011

Prevrhal, S. (2005). Quantitative Micro-CT. In F. P. Doty, H. B. Barber, & H. Roehrig (Eds.), *Proceedings of SPIE* (Vol. 5923, p. 59230K–59230K–9). doi:10.1117/12.625919

Robinson, S., Suomalainen, A., & Kortesniemi, M. (2005). Mu-CT. *European Journal of Radiology*, *56*(2), 185–191. doi:10.1016/j.ejrad.2005.03.022

Ross, M. H., & Pawlina, W. (2011). *Histology: A Text and Atlas* (sixth.). Baltimore: Lippincott, Williams, & Wilkins.

Ryu, J.-H., Park, J. H., Vu Thi Thu, T., Bayome, M., Kim, Y., & Kook, Y.-A. (2012). Palatal bone thickness compared with cone-beam computed tomography in adolescents and adults for mini-implant placement. *American Journal of Orthodontics and Dentofacial Orthopedics : Official Publication of the American Association of Orthodontists, Its Constituent Societies, and the American Board of Orthodontics*, *142*(2), 207–12. doi:10.1016/j.ajodo.2012.03.027

Sandler, J., Benson, P. E., Doyle, P., Majumder, A., O'Dwyer, J., Speight, P., … Tinsley, D. (2008). Palatal Implants are a Good Alternative to Headgear: A Randomized Trial. *American Journal of Orthodontics and Dentofacial Orthopedics*, *131*(1), 51–57.

Schätzle, M., Männchen, R., Zwahlen, M., & Lang, N. P. (2009). Survival and failure rates of orthodontic temporary anchorage devices: A systematic review. *Clinical Oral Implants Research*, *20*(12), 1351–1359. doi:10.1111/j.1600-0501.2009.01754.x

Scheid, R. C., & Weiss, G. (2012). *Woelfels Dental Anatomy* (8th ed.). Philadelphia: Lippincott, Williams, & Wilkins.

Song, W. C., Jo, D. I., Lee, J. Y., Kim, J. N., Hur, M. S., Hu, K. S., … Koh, K. S. (2009). Microanatomy of the incisive canal using three-dimensional reconstruction of microCT images: An ex vivo study. *Oral Surgery, Oral Medicine, Oral Pathology, Oral Radiology and Endodontology*, *108*(4), 583–590. doi:10.1016/j.tripleo.2009.06.036

Stockmann, P., Schlegel, K. A., Srour, S., Neukam, F. W., Fenner, M., & Felszeghy, E. (2009a). Which region of the median palate is a suitable location of temporary orthodontic anchorage devices? A histomorphometric study on human cadavers aged 15-20 years. *Clinical Oral Implants Research*, *20*(3), 306–312. doi:10.1111/j.1600-0501.2008.01647.x

Stockmann, P., Schlegel, K. A., Srour, S., Neukam, F. W., Fenner, M., & Felszeghy, E. (2009b). Which region of the median palate is a suitable location of temporary orthodontic anchorage

devices? A histomorphometric study on human cadavers aged 15-20 years. *Clinical Oral Implants Research*, *20*(3), 306–312. doi:10.1111/j.1600-0501.2008.01647.x

Swain, M. V, & Xue, J. (2009). State of the art of Micro-CT applications in dental research. *International Journal of Oral Science*, *1*(4), 177–188. doi:10.4248/IJOS09031

Wehrbein, H. (2008). Anatomic site evaluation of the palatal bone for temporary orthodontic anchorage devices. *Clinical Oral Implants Research*, *19*(7), 653–656. doi:10.1111/j.1600-0501.2008.01535.x

Wehrbein, H. (2009a). Bone quality in the midpalate for temporary anchorage devices. *Clinical Oral Implants Research*, *20*(1), 45–49. doi:10.1111/j.1600-0501.2008.01600.x

Wehrbein, H. (2009b). Bone quality in the midpalate for temporary anchorage devices. *Clinical Oral Implants Research*, *20*(1), 45–9. doi:10.1111/j.1600-0501.2008.01600.x

Wehrbein, H., Merz, B. R., & Diedrich, P. (1999). Palatal bone support for orthodontic implant anchorage — a clinical and radiological study. *European Journal of Orthodontics*, *21*, 65–70.

Wiechmann, D., Meyer, U., & Büchter, A. (2007). Success rate of mini- and micro-implants used for orthodontic anchorage: A prospective clinical study. *Clinical Oral Implants Research*, *18*(2), 263–267. doi:10.1111/j.1600-0501.2006.01325.x

Winsauer, H., Vlachojannis, C., Bumann, A., Vlachojannis, J., & Chrubasik, S. (2014). Paramedian vertical palatal bone height for mini-implant insertion: a systematic review. *European Journal of Orthodontics*, *36*(5), 541–9. doi:10.1093/ejo/cjs068

Worthy, S. (1995). High resolution computed tomography of the lungs. *British Medical Journal, 310*(6980), 615. Retrieved from http://search.proquest.com/docview/203995074?accountid=15115

Appendices

Appendix A – Permissions to Scholarship@Western

I grant, on behalf of UWO, the non-exclusive right to distribute my submission publicly as part of the University of Western Ontario Institutional Repository *Scholarship@Western.*

Appendix B - Rights and Permissions

ELSEVIER LICENSE
TERMS AND CONDITIONS

Apr 14, 2015

This is a License Agreement between Jillian N Phillips ("You") and Elsevier ("Elsevier") provided by Copyright Clearance Center ("CCC"). The license consists of your order details, the terms and conditions provided by Elsevier, and the payment terms and conditions.

All payments must be made in full to CCC. For payment instructions, please see information listed at the bottom of this form.

Supplier	Elsevier Limited The Boulevard,Langford Lane Kidlington,Oxford,OX5 1GB,UK
Registered Company Number	1982084
Customer name	Jillian N Phillips
Customer address	112 Baseline Rd W London , ON N6J2V4
License number	3607640195109
License date	Apr 14, 2015
Licensed content publisher	Elsevier
Licensed content publication	Oral Surgery, Oral Medicine, Oral Pathology, Oral Radiology, and Endodontology
Licensed content title	Microanatomy of the incisive canal using three-dimensional reconstruction of microCT images: An ex vivo study
Licensed content author	Wu-Chul Song, Dong-In Jo, Jeong-Yong Lee, Jeong-Nam Kim, Mi-Sun Hur, Kyung-Seok Hu, Hee-Jin Kim, Chuog Shin, Ki-Seok Koh
Licensed content date	October 2009
Licensed content volume number	108
Licensed content issue number	4
Number of pages	8
Start Page	583
End Page	590
Type of Use	reuse in a thesis/dissertation
Portion	figures/tables/illustrations

Number of figures/tables/illustrations	1
Format	both print and electronic
Are you the author of this Elsevier article?	No
Will you be translating?	No
Original figure numbers	Fig.2.
Title of your thesis/dissertation	A Comparative Assessment of Hard Palate Thickness using Micro-CT and Gross Cadaveric Measurements: Implications for the Safe Placement of Orthodontic Miniscrews
Expected completion date	May 2015
Estimated size (number of pages)	60
Elsevier VAT number	GB 494 6272 12
Permissions price	0.00 CAD
VAT/Local Sales Tax	0.00 CAD / 0.00 GBP
Total	0.00 CAD
Terms and Conditions	

INTRODUCTION

1. The publisher for this copyrighted material is Elsevier. By clicking "accept" in connection with completing this licensing transaction, you agree that the following terms and conditions apply to this transaction (along with the Billing and Payment terms and conditions established by Copyright Clearance Center, Inc. ("CCC"), at the time that you opened your Rightslink account and that are available at any time at http://myaccount.copyright.com).

GENERAL TERMS

2. Elsevier hereby grants you permission to reproduce the aforementioned material subject to the terms and conditions indicated.

3. Acknowledgement: If any part of the material to be used (for example, figures) has appeared in our publication with credit or acknowledgement to another source, permission must also be sought from that source. If such permission is not obtained then that material may not be included in your publication/copies. Suitable acknowledgement to the source must be made, either as a footnote or in a reference list at the end of your publication, as follows:

"Reprinted from Publication title, Vol /edition number, Author(s), Title of article / title of chapter, Pages No., Copyright (Year), with permission from Elsevier [OR APPLICABLE SOCIETY COPYRIGHT OWNER]." Also Lancet special credit - "Reprinted from The Lancet, Vol. number, Author(s), Title of article, Pages No., Copyright (Year), with permission from Elsevier."

4. Reproduction of this material is confined to the purpose and/or media for which permission is hereby given.

5. Altering/Modifying Material: Not Permitted. However figures and illustrations may be altered/adapted minimally to serve your work. Any other abbreviations, additions, deletions and/or any other alterations shall be made only with prior written authorization of Elsevier Ltd. (Please contact Elsevier at permissions@elsevier.com)

6. If the permission fee for the requested use of our material is waived in this instance, please be advised that your future requests for Elsevier materials may attract a fee.

7. Reservation of Rights: Publisher reserves all rights not specifically granted in the combination of (i) the license details provided by you and accepted in the course of this licensing transaction, (ii) these terms and conditions and (iii) CCC's Billing and Payment terms and conditions.

8. License Contingent Upon Payment: While you may exercise the rights licensed immediately upon issuance of the license at the end of the licensing process for the transaction, provided that you have disclosed complete and accurate details of your proposed use, no license is finally effective unless and until full payment is received from you (either by publisher or by CCC) as provided in CCC's Billing and Payment terms and conditions. If full payment is not received on a timely basis, then any license preliminarily granted shall be deemed automatically revoked and shall be void as if never granted. Further, in the event that you breach any of these terms and conditions or any of CCC's Billing and Payment terms and conditions, the license is automatically revoked and shall be void as if never granted. Use of materials as described in a revoked license, as well as any use of the materials beyond the scope of an unrevoked license, may constitute copyright infringement and publisher reserves the right to take any and all action to protect its copyright in the materials.

9. Warranties: Publisher makes no representations or warranties with respect to the licensed material.

10. Indemnity: You hereby indemnify and agree to hold harmless publisher and CCC, and their respective officers, directors, employees and agents, from and against any and all claims arising out of your use of the licensed material other than as specifically authorized pursuant to this license.

11. No Transfer of License: This license is personal to you and may not be sublicensed, assigned, or transferred by you to any other person without publisher's written permission.

12. No Amendment Except in Writing: This license may not be amended except in a writing signed by both parties (or, in the case of publisher, by CCC on publisher's behalf).

13. Objection to Contrary Terms: Publisher hereby objects to any terms contained in any purchase order, acknowledgment, check endorsement or other writing prepared by you, which terms are inconsistent with these terms and conditions or CCC's Billing and Payment

terms and conditions. These terms and conditions, together with CCC's Billing and Payment terms and conditions (which are incorporated herein), comprise the entire agreement between you and publisher (and CCC) concerning this licensing transaction. In the event of any conflict between your obligations established by these terms and conditions and those established by CCC's Billing and Payment terms and conditions, these terms and conditions shall control.

14. Revocation: Elsevier or Copyright Clearance Center may deny the permissions described in this License at their sole discretion, for any reason or no reason, with a full refund payable to you. Notice of such denial will be made using the contact information provided by you. Failure to receive such notice will not alter or invalidate the denial. In no event will Elsevier or Copyright Clearance Center be responsible or liable for any costs, expenses or damage incurred by you as a result of a denial of your permission request, other than a refund of the amount(s) paid by you to Elsevier and/or Copyright Clearance Center for denied permissions.

LIMITED LICENSE

The following terms and conditions apply only to specific license types:

15. **Translation**: This permission is granted for non-exclusive world **English** rights only unless your license was granted for translation rights. If you licensed translation rights you may only translate this content into the languages you requested. A professional translator must perform all translations and reproduce the content word for word preserving the integrity of the article. If this license is to re-use 1 or 2 figures then permission is granted for non-exclusive world rights in all languages.

16. **Posting licensed content on any Website**: The following terms and conditions apply as follows: Licensing material from an Elsevier journal: All content posted to the web site must maintain the copyright information line on the bottom of each image; A hyper-text must be included to the Homepage of the journal from which you are licensing at http://www.sciencedirect.com/science/journal/xxxxx or the Elsevier homepage for books at http://www.elsevier.com; Central Storage: This license does not include permission for a scanned version of the material to be stored in a central repository such as that provided by Heron/XanEdu.

Licensing material from an Elsevier book: A hyper-text link must be included to the Elsevier homepage at http://www.elsevier.com . All content posted to the web site must maintain the copyright information line on the bottom of each image.

Posting licensed content on Electronic reserve: In addition to the above the following clauses are applicable: The web site must be password-protected and made available only to bona fide students registered on a relevant course. This permission is granted for 1 year only. You may obtain a new license for future website posting.

17. **For journal authors:** the following clauses are applicable in addition to the above:

Preprints:

A preprint is an author's own write-up of research results and analysis, it has not been peer-reviewed, nor has it had any other value added to it by a publisher (such as formatting, copyright, technical enhancement etc.).

Authors can share their preprints anywhere at any time. Preprints should not be added to or enhanced in any way in order to appear more like, or to substitute for, the final versions of articles however authors can update their preprints on arXiv or RePEc with their Accepted Author Manuscript (see below).

If accepted for publication, we encourage authors to link from the preprint to their formal publication via its DOI. Millions of researchers have access to the formal publications on ScienceDirect, and so links will help users to find, access, cite and use the best available version. Please note that Cell Press, The Lancet and some society-owned have different preprint policies. Information on these policies is available on the journal homepage.

Accepted Author Manuscripts: An accepted author manuscript is the manuscript of an article that has been accepted for publication and which typically includes author-incorporated changes suggested during submission, peer review and editor-author communications.

Authors can share their accepted author manuscript:

- immediately
    - via their non-commercial person homepage or blog
    - by updating a preprint in arXiv or RePEc with the accepted manuscript
    - via their research institute or institutional repository for internal institutional uses or as part of an invitation-only research collaboration work-group
    - directly by providing copies to their students or to research collaborators for their personal use
    - for private scholarly sharing as part of an invitation-only work group on commercial sites with which Elsevier has an agreement
- after the embargo period
    - via non-commercial hosting platforms such as their institutional repository
    - via commercial sites with which Elsevier has an agreement

In all cases accepted manuscripts should:

- link to the formal publication via its DOI

- bear a CC-BY-NC-ND license - this is easy to do

- if aggregated with other manuscripts, for example in a repository or other site, be shared in alignment with our hosting policy not be added to or enhanced in any way to appear more like, or to substitute for, the published journal article.

Published journal article (JPA): A published journal article (PJA) is the definitive final record of published research that appears or will appear in the journal and embodies all value-adding publishing activities including peer review co-ordination, copy-editing, formatting, (if relevant) pagination and online enrichment.

Policies for sharing publishing journal articles differ for subscription and gold open access articles:

Subscription Articles: If you are an author, please share a link to your article rather than the full-text. Millions of researchers have access to the formal publications on ScienceDirect, and so links will help your users to find, access, cite, and use the best available version.

Theses and dissertations which contain embedded PJAs as part of the formal submission can be posted publicly by the awarding institution with DOI links back to the formal publications on ScienceDirect.

If you are affiliated with a library that subscribes to ScienceDirect you have additional private sharing rights for others' research accessed under that agreement. This includes use for classroom teaching and internal training at the institution (including use in course packs and courseware programs), and inclusion of the article for grant funding purposes.

Gold Open Access Articles: May be shared according to the author-selected end-user license and should contain a CrossMark logo, the end user license, and a DOI link to the formal publication on ScienceDirect.

Please refer to Elsevier's posting policy for further information.

18. **For book authors** the following clauses are applicable in addition to the above: Authors are permitted to place a brief summary of their work online only. You are not allowed to download and post the published electronic version of your chapter, nor may you scan the printed edition to create an electronic version. **Posting to a repository:** Authors are permitted to post a summary of their chapter only in their institution's repository.

19. **Thesis/Dissertation**: If your license is for use in a thesis/dissertation your thesis may be submitted to your institution in either print or electronic form. Should your thesis be published commercially, please reapply for permission. These requirements include permission for the Library and Archives of Canada to supply single copies, on demand, of the complete thesis and include permission for Proquest/UMI to supply single copies, on demand, of the complete thesis. Should your thesis be published commercially, please reapply for permission. Theses and dissertations which contain embedded PJAs as part of the formal submission can be posted publicly by the awarding institution with DOI links back to the formal publications on ScienceDirect.

Commercial reuse includes:

- Associating advertising with the full text of the Article
- Charging fees for document delivery or access
- Article aggregation
- Systematic distribution via e-mail lists or share buttons

Posting or linking by commercial companies for use by customers of those companies.

20. **Other Conditions**:

Wolters Kluwer

5/04/2015

Jillian Phillips
University of Western Ontario

Re: Moore: Essential Clinical Anatomy 4e. p561 Figure: 7-54B.
Re: Scheid: Woelfel's Dental Anatomy 8e. Figures 15-21 and 15-22.
Spec Material: Thesis: Comparative Assessment of Hard Palate Thickness Using Micro-CT and Gross Cadaveric...
Format: Print and electronic.
Request No.: 150412-000310.

Wolters Kluwer Terms and Conditions

1. A credit line will be prominently placed and include: the author(s), title of book, edition, copyright holder, year of publication.
2. The requestor warrants that the material shall not be used in any manner which may be considered derogatory to the title, content, or authors of the material, or to Wolters Kluwer.
3. Permission is granted for a one time use only. Rights herein do not apply to future reproductions, editions, revisions, or other derivative works.
4. Permission granted is non-exclusive, and is valid throughout the world in the English language and the languages specified in your original request.
5. Wolters Kluwer cannot supply the requestor with the original artwork, clean copy, or electronic file(s) for figures.
6. Permission is valid if the borrowed material is original to a Wolters Kluwer imprint (Lippincott Williams & Wilkins, Lippincott-Raven Publishers, Williams & Wilkins, Lea & Febiger, Harwal, Rapid Science, Little Brown & Company, Harper & Row Medical, American Journal of Nursing Co, and Urban & Schwarzenberg - English Language).
7. If you opt not to use the material requested above, please notify Wolters Kluwer within 90 days of the original invoice date.
8. This permission does not apply to images/tables/content that are credited to publications other than Wolters Kluwer books. For images credited to non-Wolters Kluwer books, you will need to obtain permission from the source referenced in the figure or table legend or credit line before making any use of the image(s), table(s) or other content.
9. Adaptations are protected by copyright, so if you would like to reuse material that we have adapted from another source, you will need not only our permission, but the permission of the rights holder of the original material. Similarly, if you want to reuse an adaptation of original Wolters Kluwer content that appears in another publisher's work, you will need our permission and that of the next publisher. The adaptation should be credited as follows: Adapted with permission from Wolters Kluwer: book author, title, year of publication.
10. Please note that modification of text within figures or full-text article is strictly forbidden.

Please retain this license for your files.

Sincerely,

Wolters Kluwer Book Permissions Group

Appendix C: Specimen Information

Specimen ID	Age	Sex	Medical Information
1513	78	M	Cardiac Arrest, Pulmonary Edema, Cardiogenic Shock, Myocardial Infarction, Chronic Renal Failure.
1517	86	M	Myocardial Infarction, CAD, CHF, Acute Renal Failure
1576	57	M	Prostate Cancer
1589	98	M	ASHD, Atrial Fibrillation, CHF, Peripheral Vascular Disease
1605	54	M	Aspiration Pneumonia, Huntington's Chorea
1615	80	M	Complications of Lung Injury from MVC, Pneumonia, ARDS, Rib Fracture, Pneumothorax, Pulmonary Embolus, CHF, CAD
1672	93	F	End Stage Dementia, CVA, Hypertension
1683	93	F	Cardiorespiratory Failure, CHF
1706	61	M	Hepatic Failure, Alcoholic Liver Cirrhosis
1719	76	F	Pneumonia, Pulmonary Fibrosis, Methotrexate Usage, Giant Cell Arteritis

Appendix D: Sites Extended with a 12mm OMS

Specimen ID	Sites Extended
1513	L2, S1
1576	PS1, LS, S1
1589	S1
1605	PS1
1615	PS1, S1
1706	PS1
1719	PS1, L2

Appendix E: Averaged Measurements and Percent Errors for Validation Study

		Average Calliper Measurement (mm)	Average Pin Measurement (mm)		Percent Error (%) Between Measurements
Wood Block	Site	Average Thickness (mm)	Site	Average Depth (mm)	
V1	1	12.25	1	12.38	1.04
V1	2	8.76	2	8.67	-1.06
V1	3	6.44	3	6.24	-3.11
V1	4	4.03	4	4.07	1.12
V1	5	2.64	5	2.73	3.41
V1	6	1.74	6	1.75	0.43
V2	1	11.32	1	11.16	-1.44
V2	2	7.30	2	7.35	0.65
V2	3	4.86	3	4.78	1.54
V2	4	3.048	4	3.11	1.97
V2	5	2.17	5	2.31	6.69
V2	6	1.61	6	1.70	5.44
V3	1	12.02	1	11.90	-1.02
V3	2	8.00	2	8.03	0.34
V3	3	5.54	3	5.52	0.50
V3	4	3.79	4	3.95	4.16
V3	5	2.81	5	2.92	3.92
V3	6	1.81	6	1.80	0.14
V4	1	9.80	1	9.53	2.71
V4	2	5.75	2	5.81	1.04
V4	3	4.30	3	4.37	1.63
V4	4	3.37	4	3.33	1.19
V4	5	2.15	5	2.25	5.01
V4	6	1.60	6	1.6475	3.13
V4	1	10.09	1	10.33	2.33
V5	2	6.12	2	5.92	-3.3
V5	3	3.75	3	3.72	0.47
V5	4	2.27	4	2.23	1.77
V5	5	1.75	5	1.85	5.87
V5	6	1.59	6	1.63	2.83

Appendix F: Bone Thickness Measurements

		Rater One			Rater Two	Micro-CT BT (mm)
Specimen ID	**Site**	**Physical BT (mm) Trial 1**	**Physical BT (mm) Trial 2**	**Avg. Physical BT (mm)**	**Physical BT (mm)**	
1513	PS1	6.76	6.62	6.69	7.48	5.3088
1513	S1					9.5411
1513	PS2	3.53	3.50	3.52	2.82	4.0679
1513	S2	3.40	3.30	3.35	3.33	3.3854
1513	L2					6.6935
1513	PS3	3.61	3.78	3.70	3.91	4.6935
1513	S3	2.11	2.05	2.08	2.13	1.9235
1513	L3	2.89	3.18	3.04	2.87	3.3085
1513	PS4	3.57	3.44	3.51	3.76	3.5393
1513	S4	1.70	1.56	1.63	1.71	1.385
1513	L4	2.75	2.24	2.50	2.42	2.2313
1513	PS5	2.25	1.98	2.12	3.52	1.8466
1513	S5	1.59	1.41	1.50	2.44	1.5388
1517	PS1					7.5404
1517	S1	4.25	4.32	4.29	4.12	8.6942
1517	PS2	4.42	4.56	4.49	4.11	7.4635
1517	S2	4.40	4.41	4.41	4.06	4.3087
1517	L2	2.82	2.28	2.55	3.17	3.8471
1517	PS3	4.76	4.74	4.75	4.47	4.9243
1517	S3	3.54	3.19	3.37	3.09	3.3085
1517	L3	3.36	3.23	3.30	3.12	2.8468
1517	PS4	5.22	4.91	5.07	4.67	4.7704
1517	S4	1.95	1.92	1.94	1.63	2.2313
1517	L4	2.03	2.20	2.12	2.16	1.7696
1517	PS5	2.33	2.51	2.42	1.91	2.616
1517	S5	1.87	1.89	1.88	1.35	1.5388
1576	PS1					11.695
1576	S1					10.2331
1576	PS2	5.07	4.72	4.90	4.85	4.7704
1576	S2	3.87	3.78	3.83	4.12	4.001
1576	L2					8.3101
1576	PS3	3.57	3.66	3.62	3.45	3.924

1576	S3	1.97	2.04	2.01	2.81	2.0005
1576	L3	3.07	3.28	3.18	2.85	4.2318
1576	PS4	2.44	2.55	2.50	2.51	2.6929
1576	S4	1.45	1.19	1.32	1.88	1.5388
1576	L4	0.82	0.57	0.70	1.83	1.0002
1576	PS5	4.13	4.17	4.15	4.85	3.7702
1576	S5	0.66	0.73	0.70	1.65	0.6924
1589	PS1	8.58	8.45	8.52	8.56	7.617
1589	S1					9.1562
1589	PS2	3.96	3.83	3.90	4.03	3.8465
1589	S2	3.08	2.76	2.92	3.29	2.9238
1589	L2	3.47	3.8	3.64	3.74	5.4628
1589	PS3	3.49	3.42	3.46	3.54	3.0007
1589	S3	1.96	1.98	1.97	2.08	2.0005
1589	L3	4.67	4.59	4.63	4.77	5.5394
1589	PS4	3.90	3.41	3.66	4.16	5.0012
1589	S4	1.82	1.65	1.74	1.57	1.5388
1589	L4	1.38	1.09	1.24	1.45	1.0771
1589	PS5	2.14	2.14	2.14	2.39	1.8466
1589	S5	1.22	0.92	1.07	1.25	1.0772
1605	PS1	8.02	8.25	8.14	8.27	7.156
1605	S1	9.18	8.95	9.07	9.50	8.848
1605	PS2	4.03	5.03	4.53	4.99	5.1547
1605	S2	3.89	3.88	3.89	3.35	3.5394
1605	L2	7.79	7.48	7.64	10.01	6.2321
1605	PS3	3.60	3.64	3.62	3.52	3.3085
1605	S3	2.04	1.96	2.00	2.15	2.3083
1605	L3	0.56	0.62	0.59	0.76	1.0772
1605	PS4	2.84	3.88	3.36	2.64	5.6939
1605	S4	1.17	1.18	1.18	1.61	0.9233
1605	L4	1.81	1.83	1.82	1.65	1.8466
1605	PS5	2.23	2.45	2.34	2.86	2.4621
1605	S5	1.62	1.71	1.67	1.83	1.7697
1615	PS1					10.7719
1615	S1					11.1564
1615	PS2	5.38	5.18	5.28	5.20	5.8475
1615	S2	4.76	4.85	4.81	4.69	5.4626
1615	L2	6.84	6.57	6.71	7.06	6.07844

1615	PS3	4.24	3.92	4.08	4.58	4.3087
1615	S3	1.47	1.61	1.54	3.02	1.5319
1615	L3	2.28	2.50	2.39	2.79	2.0774
1615	PS4	2.50	2.63	2.57	2.40	2.3852
1615	S4	1.25	1.14	1.20	1.65	1.0772
1615	L4					0.5386
1615	PS5	3.97	3.83	3.90	4.32	4.001
1615	S5	0.71	0.98	0.85	1.20	0.7694
1672	PS1	6.84	6.52	6.68	7.14	6.3092
1672	S1	6.52	6.49	6.51	6.18	7.3861
1672	PS2	3.69	3.99	3.84	3.65	3.6163
1672	S2	1.38	1.56	1.47	1.85	1.5389
1672	L2	4.14	3.81	3.98	3.70	4.001
1672	PS3	2.24	2.66	2.45	2.96	2.693
1672	S3	1.30	0.85	1.08	1.24	1.0002
1672	L3	0.71	0.68	0.70	0.72	0.6925
1672	PS4	2.73	2.78	2.76	2.57	2.616
1672	S4	0.62	0.54	0.58	1.53	0.8464
1672	L4	0.37	0.33	0.35	1.09	0.4617
1672	PS5	1.82	1.79	1.81	2.16	1.6927
1672	S5	0.53	0.59	0.56	1.41	0.5386
1683	PS1	1.17	1.17	1.17	1.63	1.308
1683	S1	2.10	1.88	1.99	1.72	1.7697
1683	PS2	2.03	1.89	1.96	2.16	5.0013
1683	S2	0.65	0.49	0.57	0.55	0.8464
1683	L2	1.30	1.27	1.29	1.36	1.2311
1683	PS3	2.29	2.24	2.27	2.15	2.6929
1683	S3	0.53	0.50	0.52	0.64	0.7694
1683	L3	1.42	1.42	1.42	1.64	1.5388
1683	PS4	2.88	2.89	2.89	2.14	3.4624
1683	S4	0.37	0.38	0.38	0.85	0.4617
1683	L4	0.76	0.74	0.75	0.74	1.0003
1683	PS5	2.20	2.37	2.29	2.30	0.9233
1683	S5	0.69	0.78	0.74	0.74	0.8463
1706	PS1					10.9261
1706	S1	9.95	9.91	9.93	10.25	11.1563
1706	PS2	4.29	4.29	4.29	3.86	3.7702
1706	S2	4.18	4.21	4.20	4.10	3.9241

1706	L2	5.84	5.54	5.69	8.20	6.3097
1706	PS3	2.45	2.49	2.47	2.43	2.4622
1706	S3	2.19	2.40	2.30	2.12	2.3082
1706	L3	3.50	3.47	3.49	3.65	3.5393
1706	PS4	4.09	4.04	4.07	3.81	4.3857
1706	S4	1.58	1.73	1.66	2.32	1.8466
1706	L4	1.75	1.80	1.78	1.30	2.1543
1706	PS5	2.83	2.94	2.89	2.96	2.8469
1706	S5	1.53	1.70	1.62	1.96	1.5388
1719	PS1					10.156
1719	S1	10.47	10.57	10.52	10.56	10.233
1719	PS2	3.40	3.32	3.36	3.02	3.2316
1719	S2	2.70	3.00	2.85	2.54	6.6171
1719	L2					7.617
1719	PS3	2.88	2.88	2.88	2.61	2.1544
1719	S3	0.53	0.59	0.56	0.95	0.6924
1719	L3	1.00	1.63	1.32	1.80	1.5389
1719	PS4	2.34	2.24	2.29	1.85	2.5391
1719	S4					1.2311
1719	L4	0.35	0.50	0.43	0.69	0.6155
1719	PS5	3.13	3.06	3.10	3.24	2.6929
1719	S5	0.93	0.83	0.88	1.25	0.8463

* Blank values represent sites at which physical BT measurements were excluded due to bone fracture or need for additional dissection that could introduce errors in measurements.

Appendix G: SPSS® Output - Tests of Normality

Tests of Normality

		Kolmogorov-Smirnov[a]			Shapiro-Wilk		
	Site	Statistic	df	Sig.	Statistic	df	Sig.
Difference btwn physical BT measurement and micro-CT	L2	.148	7	.200*	.983	7	.974
	L3	.169	10	.200*	.951	10	.686
	L4	.144	9	.200*	.935	9	.529
	PS1	.233	5	.200*	.961	5	.816
	PS2	.314	10	.006	.757	10	.004
	PS3	.170	10	.200*	.963	10	.819
	PS4	.261	10	.053	.813	10	.021
	PS5	.262	10	.051	.808	10	.018
	S1	.276	6	.171	.761	6	.025
	S2	.350	10	.001	.584	10	.000
	S3	.236	10	.120	.920	10	.357
	S4	.207	9	.200*	.858	9	.091
	S5	.255	10	.064	.836	10	.039

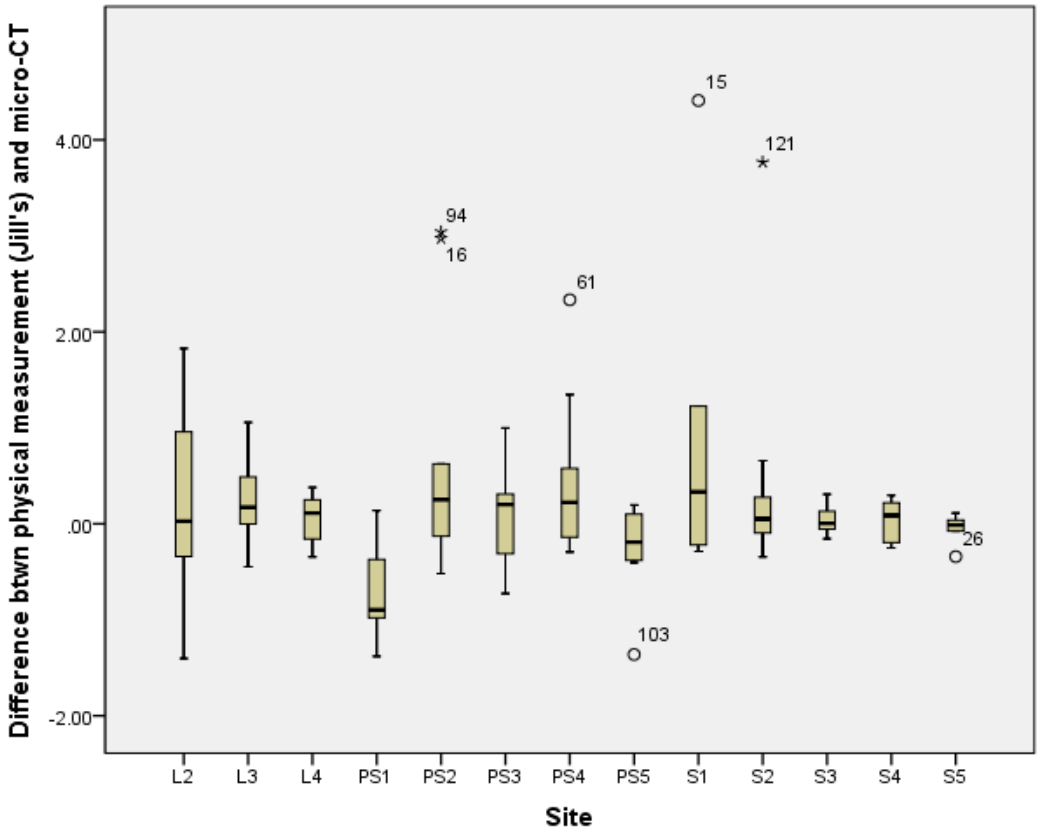

Box and Whisker Plots Representing Distribution of Measurements Differences By Site

Appendix H: SPSS® Output - Kruskall Wallis H test

Hypothesis Test Summary

	Null Hypothesis	Test	Sig.	Decision
1	The distribution of Difference btwn physical measurement (Jill's) and micro-CT is the same across categories of Site.	Independent-Samples Kruskal-Wallis Test	.195	Retain the null hypothesis.

Asymptotic significances are displayed. The significance level is .05.

Independent-Samples Kruskal-Wallis Test

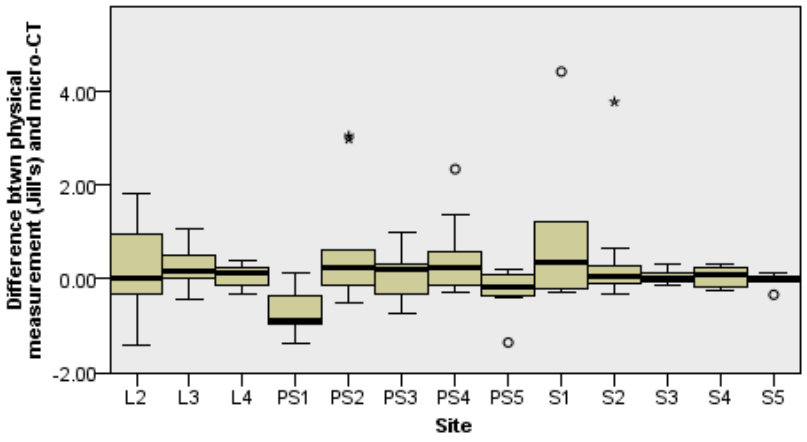

Total N	116
Test Statistic	15.910
Degrees of Freedom	12
Asymptotic Sig. (2-sided test)	.195

1. The test statistic is adjusted for ties.
2. Multiple comparisons are not performed because the overall test does not show significant differences across samples.

Curriculum Vitae

EDUCATION

Masters of Science in Clinical Anatomy **June, 2015**
Western University (formerly: The University of Western Ontario), London, ON, Canada

Bachelor of Science, Majors in Biology and Psychology **May, 2013**
Saint Mary's University, Halifax, NS, Canada

TEACHING EXPERIENCE

Guest Lecturer, Systemic Anatomy (ACB 3319) **October 21, 2014**
Teaching Assistant, Online Histology (ACB 3309) **Sept. 1, 2014 –April 30, 2015**
Laboratory Teaching Assistant, Undergraduate Medicine **Sept. 1, 2014 – April 24, 2015**
Teaching Assistant for Online Histology **Sept. 1, 2013 – April 30, 2014**
Teaching Assistant for Systemic Anatomy **Sept. 1, 2013 – April 30, 2014**

PROFESSIONAL DEVELOPMENT, WESTERN UNIVERSITY

Certificate in University Teaching and Learning **March 2015**
Western Teaching Support Center

Putting Together a Teaching Dossier	**October 29, 2013**
Writing A Teaching Philosophy Statement	**October 29, 2013**
Career Workshop: Successes & Challenges of Non-Academic Careers in Science	**January 2014**
Winter Conference on Teaching for Graduate Students	**January 2014**
Spring Perspectives on Teaching Conference	**May 2014**
Using Social Media Effectively in the University Classroom	**June 26, 2014**
How to Get and Use Student Feedback to Improve Learning During the Term	**August 27, 2014**
Putting Together a Teaching Dossier	**October 29, 2013**
Writing A Teaching Philosophy Statement	**October 29, 2013**
Winter Conference on Teaching for Graduate Students	**January 2014**
Spring Perspectives on Teaching Conference	**May 2014**
Using Social Media Effectively in the University Classroom	**June 26, 2014**
How to Get and Use Student Feedback to Improve Learning During the Term	**August 27, 2014**

RESEARCH POSTER PRESENTATIONS

AAA Annual Meeting at Experimental Biology **March 31, 2015**
- Travel Award Recipient

Anatomy and Cell Biology Research Day, *Western University* **October 23, 2014**

Schulich Annual Dentistry Research Day, *Western University* **October 8, 2014**
Poster Finalist, Senior Category

COMMUNITY INVOLVEMENT

Gross Anatomy Lab Volunteer **December 2013- Present**
Western University, London Ontario, Canada

- Foot and ankle session (**Sept. 2015**)
- Thigh, leg, foot anatomy refresher session for MPT. Students (**Feb. 2015**)
- Brain and spinal cord anatomy demonstration for high school students (**Dec. 2014**)
- Human osteology demonstration for high school students (**Dec. 2013)**

Let's Talk Science Outreach Volunteer: UWO Chapter **Sept. 2014 – Present**
Teacher Partnership with Ms. Claire Gulliver, Jack Chambers Public School, London Ontario

Community Member Interviewer for 2014 Dental Student Applicants **April 2014**
Western University, London Ontario, Canada

Volunteer Usher, BMSc. Convocation **June 12, 2014**
Western University, London Ontario, Canada

Let's Talk Science Outreach Volunteer: UWO Chapter **Sept. 2013 – June 2014**
Teacher Partnership with Mrs. K. McArthur, Stoney Creek Public School, London Ontario

RELEVANT EMPLOYMENT EXPERIENCE

Anatomy Prosector Summer Studentship **July 2014-August 2014**
Dalhousie University, Halifax, NS, Canada